Solar-assisted integrated biogas solid oxide fuel cell (SOFC) installation in wastewater treatment plant: Energy and economic analysis

Solar-assisted integrated biogas solid oxide fuel cell (SOFC) installation in wastewater treatment plant: energy and economic analysis

A. S. Mehr[1], M. Gandiglio[2*], M. MosayebNezhad[2], A. Lanzini[2], S.M.S. Mahmoudi[1], M. Yari[1], M. Santarelli[2]

1. Faculty of Mechanical Engineering. University of Tabriz, Tabriz, Iran
2. Department of Energy, Politecnico di Torino, Turin, Italy

Abstract

A unique cogeneration system integrating a biogas fed Solid Oxide Fuel Cell (SOFC) and a Concentrating Solar Thermal (CST) system for a reference Waste Water Treatment Plant (WWTP) in Italy is proposed. Biogas – which is locally in the WWTP from the anaerobic digestion (AD) of the collected sludge – can be used to produce electricity using SOFC power modules. The thermal power recovered from the SOFC exhaust stream is used to meet part of the digester thermal load. However, the rest heat loads are provided by using the integration with the CST system and an auxiliary boiler. Energy analysis is performed to determine the effect of using the solar heating system on the system performance. Also, the economic performance is evaluated through a cash-flow analysis and the calculation of the Levelized cost of electricity (LCOE). It is observed that installing 300 m^2, 700 m^2, 1100 m^2 of solar collectors could cover 8%, 18% and 30% of total digester heat load, respectively. Results show an overall beneficial effect of the solar installation, both from an energy and economic standpoint of view. For all the scenarios analyzed, the LCOE is lower than the grid electricity price and, with increasing solar integration, the value is further reduced showing that, despite the investment return time, the electricity production during the entire system lifetime is competitive against grid electricity prices.

Keywords: *Solid Oxide Fuel Cell, Heat recovery, Solar energy, WWTP, biogas, economic analysis.*

***Corresponding author**
marta.gandiglio@polito.it

Nomenclature

Acronyms and abbreviations

AB= After Burner
AC = Alternate Current
AD = Anaerobic Digestion
c_i = cost of the component *i*, $
CAPEX = CAPital EXpenditure
CHP = Combined Heat and Power
CS = Carbon Steel
CST = Concentrating Solar thermal
DC = Direct Current
ex = exhaust
GHG = GreenHouse Gas
Inv = Investment
HRT = Hydraulic Retention Time
HX = Heat eXchanger
in = inlet
NG = *N*atural Gas
Ni = Nichel
LCOE = Levelized Cost Of Electricity
Op = Operation
out = outlet
OPEX = OPerational EXpenditure
PBT = Pay-Back Time
PrV = Production Volumes, MW/yr
PR_{ratio} =Pre-reformer Methane conversion ratio
SOFC = Solid Oxide Fuel Cell
SS = Stainless Steel
VOC = Volatile Organic Compound
WGS = Water Gas Shift
WWTP= Waste Water Treatment Plant
YSZ = Yttria Stabilized Zirconia

Parameters

T = temperature, K or °C
V = voltage, V
W = electric power, kW
c = specific heat, kJ kg-1 K-1
$\bar{h}$ = molar enthalpy, kJ kg^{-1}
LHV = lower heating value, kJ kg^{-1}
p = pressure, bar or Pa
$\bar{s}$= molar entropy, kJ kg^{-1} K^{-1}
T = temperature, K or °C
V = voltage, V
$\dot{V}$ = biogas volumetric flow rate, m3/day
W = electric power, kW

1. Introduction

Climate change and rising public consciousness for environmental protection along with the scarcity of primary energy resources have motivated researchers and policymakers to look for efficient power generation, renewable energy sources and sustainability. According to the Energy Roadmap 2050, renewable power generation in Europe will move to the center of energy supply [1]. In 2030, all the de-carbonization scenarios suggest rising shares of renewables of around 30% in gross final energy consumption. Further to this consideration, small-scale power generation systems such as wind turbines, photovoltaics, microturbines and fuel cells offer significant potential for saving energy, reducing CO_2 emissions and secure energy production.

While the vast majority of methane used in the globe today comes in the form of natural gas (NG), there is rapidly growing interest in capturing the methane formed from anaerobic digestion (AD). Anaerobic digestion is a biological process in which biodegradable organic matter such as wastewater, animal waste, food waste, or landfills is broken down by micro-organisms in the absence of oxygen into biogas consisting of methane (CH_4), carbon dioxide (CO_2), and trace amounts of other gasses. Biogas produced in an anaerobic digester is a combustible mixture, and it will become a valuable commodity when it is properly handled. The biogas from wastewater typically consists of 60-70 vol. % CH_4, 30-40 vol. % CO_2, and 1-2 vol. % N_2, and can be used as a fuel for cogeneration systems such as reciprocating engines, microturbines, or fuel cells. Several impurities are also found in biogas, mostly H_2S and siloxanes, which can damage the end-user device and thus must be removed [2–4].

Therefore, the electricity generated can offset most of a WWTP's electric power demand, and the recovered thermal energy can be used to meet digester heat load and facility space heating requirements [5–7]. Currently, most biogas, when not sent to CHP, is used to heat digesters or

- because methane content is a significant contributor to global warming - is flared in the case of surplus [8]. The biogas composition of the SMAT Collegno is given in Table 1. We use the Collegno WWTP and available data on biogas production and thermal/electric loads as the case study of this work. The plant is located in Torino (IT) and collects mixed industrial and urban wastewater for a fraction of the Torino municipality.

Table 1 Characteristics of Anaerobic Digester Gas.

Item or Parameter	Unit	Average values (reference WWTP used in this study)
Methane, CH_4	%	63.9
Carbon dioxide, CO_2	%	33.3
Oxygen, O_2	%	0.1
Hydrogen, H_2	ppm	100
Carbon Monoxide, CO	mg/m^3	1.4
Nitrogen, N_2 (calculated)	mg/m^3	2.6
Ammonia, NH_3	mg/m^3	0.1
Hydrogen sulfide, H_2S	mg/m^3	26.0
Sulphur – Mercaptans	mg/m^3	2.1
Total siloxanes	mg/m^3	14.4
Specific gravity (based on air = 1.0) [5]		0.8 – 1.0
Lower heating value, LHV [5]	MJ/m^3	19-21.6

Among the various types of fuel cells available, high temperature fuel cells such as solid oxide fuel cells (SOFCs) and molten carbonate fuel cells (MCFCs) are key candidates for integration with WWTPs. The most notable advantage of high temperature fuel cells compared with the existing fuel cell technologies is the possibility of using conventional fuels such as natural gas, diesel fuel, and biogas, instead of hydrogen. The MCFC technology is already commercially available for large power generation plants on kW and MW scale [9], while the solid oxide fuel cell (SOFC) continues its development and shortly will be ready for long-term commercial use [7,8]. Multi-generation energy systems based on fuel cells were proposed by Margalef et al. [12,13] investigating on methane-fueled SOFC plants able to produce electrical power, heat, and hydrogen.

Numerous studies have been reported on the utilization of fuel cells as CHP systems in WWTP with different configurations. Sanchez et al. [14] proposed a multi-generation system based on MCFCs and reciprocating engines in WWTPs. In their work, an MCFC is set downstream of a reciprocating engine fed by as-produced biogas. A 250 kW electric tri-generation plant based on an MCFC was operating at the Orange County Sanitation District (OCSD) in Irvine, California. The MCFC produces electricity, hydrogen and heat from the anaerobic digester gas from sludge collected in the OCSD wastewater treatment plant [15]. Trendewicz and Braun [16] conducted a comprehensive techno-economic analysis of the SOFC-based combined heat and power system for biogas utilization at wastewater treatment facilities.

Borello et al. [17] modeled an SOFC based CHP system fed by biogas produced from anaerobic digestion of organic fraction of municipal solid waste integrated with solar collectors and a thermal storage unit. The results of their transient model revealed that the heat supplied to the digester by the solar field would save 7.63 ton/y of biogas or the 4% of the total biogas production, equal to 131 GJ/y of electricity production by the SOFC. Several studies and experiments have also been dedicated to testing the performance of biogas-fed SOFC and MCFC systems. De Arespacochaga et al. [18] operated a 2.8 kW_e biogas powered SOFC for 700 hours at pilot-scale in a WWTP. Papurello et al. [19] investigated the performance of an SOFC short stack fed by biogas, showing the feasibility of the integration of H_2S-contaminaed biogas stream with fuel cell systemthatn include a sulfr trap upstream from the stack. Papurello et al. [20] have also tested a 500 W_e SOFC stack using biogas from organic waste for 400 hours. Buonomano et al. [21] tested a 1 kW MCFC with landfill biogas that was externally reformed. Chiodo et al. [22] have also analyzed the performance of different reformer SOFC configuration showing how steam reforming is the best option from a thermodynamic point view.

Recently, the SOFC technology has also been tested and demonstrated at a proof of concept level in the SOFCOM project [23]. SOFCOM was a Fuel Cell & Hydrogen Joint Undertaking (FCH-JU) funded research project aimed to demonstrate the technical feasibility, efficiency and environmental advantages of CHP plants based on SOFC fed by different typologies of biogenous primary fuels, also integrated by a process for the CO_2 separation from the anode exhaust gasses [23]. Further technical explanations about this plant as well as detailed data about its operating conditions can also be found in Ref. [24].

As mentioned above, biogas-fed SOFC power plants have attracted increasing attention in recent years. However, few works focused on the thermal integration of the biogas fueled SOFC system in WWTPs, which will be one of our most significant concerns in the present work. The research, which sets out a framework to give further details about the design and the performance of a reference biogas fed SOFC plant with emphasize on heat recovery and thermal integration of the plant, actually is a part of an EU project, namely DEMOSOFC project. DEMOSOFC [25] is an FCH-JU funded project which foresees the installation of the largest biogas fed Solid Oxide Fuel Cell (SOFC) in Europe. The SOFC will be the sole CHP generator within a medium-sized wastewater treatment plant located in the North-West of Italy (Figure 1). The WWTP serves 270’000 equivalent inhabitants collecting an average of 38’500 m^3 of wastewater on a daily basis, which corresponds to ~220 liters/day/capita. In the present work, updated real data taken from the WWTP mentioned above (SMAT Co.) are used.

The paper begins with a brief explanation of the reference WWTP including the description of the proposed CHP plant. The proposed plant is based on three solid oxide fuel cell units consuming as-produced biogas by anaerobic digestion of wastewater. Thermal integration system has the responsibility of providing the digester heat load. For the base case scenario, the thermal integration system comprises of two main loops. In the first loop, heating up sludge

comprises of three heat exchangers, which recover available heat in the exhaust gasses of the SOFC units. The second loop, which is a conventional way of sludge heating in WWTPs, comprises of a boiler which is embedded to provide required thermal load for digestion process when the recovered heat from SOFC units is not sufficient to warm up digester (the boiler can be fed either with surplus biogas or natural gas from the grid). Utilizing a parabolic trough concentrating solar thermal power system, a novel thermal integration system is proposed. In this new scenario, the solar system is integrated into parallel and series with the boiler loop. The proposed scenarios are analyzed by modeling the plants in the EES software. Feasibility of using the solar system in the plant and its effect on the system performance are evaluated. In the present work, the thermal integration, for which some conventional configurations could be proposed, is a novel scenario using a concentration solar thermal system integrated with SOFC system. Likewise, the economic evaluation is performed for the entire system including the biogas clean-up system, the SOFC units as well as the thermal heat recovery integrated with CST system.

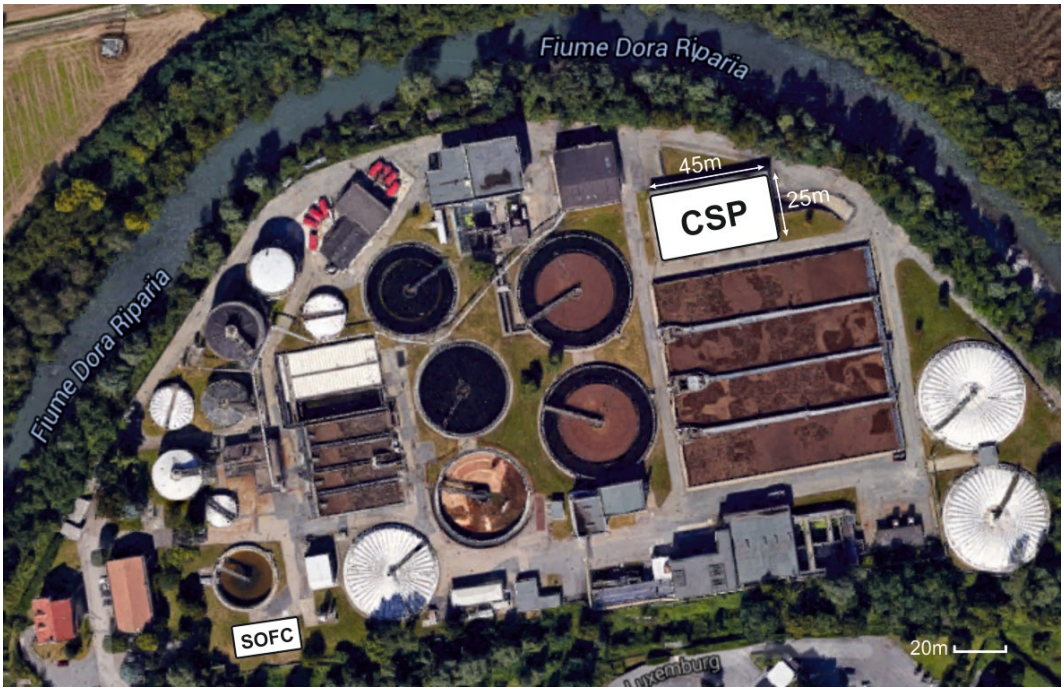

Figure 1. SMAT waste water treatment plant in Collegno (Turin). "SOFC" shows the area where the three SOFC modules will be installed. "CST" is the proposed area for the solar thermal system.

2. System layout descriptions

2.1 Wastewater treatment plants

Wastewater treatment plants are facilities dedicated to municipal wastewater treatment. Common processes found at municipal water waste treatment plants include [26]:

Preliminary treatment aims to remove large or hard solids that might clog or damage other equipment. These might include grinders, bar screens, and grit channels. The first chops up rags and trash; the second simply catches large objects, which can be raked off; the third allows heavier materials, like sand and stones, to settle out, so that they will not cause abrasive wear on downstream equipment. Grit channels also remove larger food particles (i.e., garbage).

Primary settling basins, where the water flows slowly for up to a few hours, to allow organic suspended matter to settle out or float to the surface. Most of this material has a density not much different from that of water, so it needs to be given enough time to separate. Settling tanks can be rectangular or circular. In either type, the tank needs to be designed with some scrapers at the bottom to collect the settled sludge and direct it to a pit from which it can be pumped for further treatment and skimmers at the surface, to collect the material that floats to the top.

Secondary treatment, usually biological, tries to remove the remaining dissolved or colloidal organic matter. The biodegradation of the pollutants is allowed to take place in a location where plenty of air can be supplied to the microorganisms. This promotes the formation of the less offensive, oxidized products.

Engineers try to design the capacity of the treatment units so that enough of the impurities will be removed to prevent significant oxygen demand in the receiving water after discharge.

Disinfection, usually the final process before discharge, is the destruction of harmful microorganisms, i.e. disease-causing germs. The object is not to kill every living microorganism in the water - which would be sterilization - but to reduce the number of harmful ones to levels appropriate for the intended use of the receiving water.

The most commonly used disinfectants are chlorine, ozone, and ultraviolet light. However, ultraviolet disinfection is becoming more popular because of the environmental issues associated with the use of chlorine and ozone.

Figure 2 illustrates a basic layout of the proposed wastewater treatment plant together with CHP system for two different configurations: A conventional layout (excluded the dashed line), and a novel configuration (included the dashed line) which is equipped with concentrated solar power (CST) system.

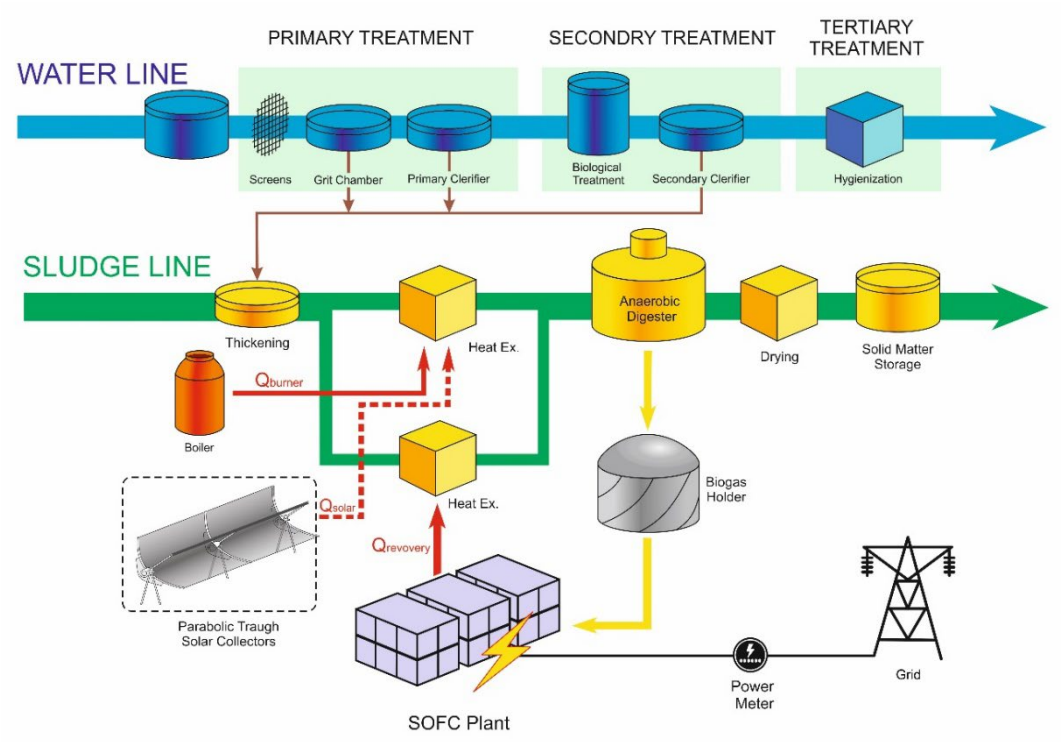

Figure 2. Proposed plant layout without CST system and with CST system (including dashed line).

2.2. Biogas production and clean-up in WWTP

The sediments precipitated from the first, and secondary treatments are collected in a tank. Sediments are semisolid materials also called sludge which is later treated physically and biologically in anaerobic digesters to reduce the organic fraction and stabilize the stream. Biogas is also obtained as a by-product of anaerobic digestion together with stabilized digested sludge. As-produced biogas consists of methane and carbon dioxide with trace amounts of fuel contaminants. This biogas is usually employed either to thermally support the digesters (by burning it into boilers) or to run cogeneration systems to produce electricity, thus reducing the power consumption of the WWTP.

Data on biogas production and plant loads (electrical and thermal) are those of the reference WWTP used in this study. The yearly biogas production trend from anaerobic digestion shows a reduction during the summer season (especially during August) resulting in the risk of biogas shortages so that, not only is biogas less for heating up digester but also there will be a problem feeding SOFC units . Both biogas production profiles of 2014 (not shown) and 2015 confirm this trend. Especially in August, less wastewater is produced (and so collected) in the urban area and thus less biogas is generated.

Due to the low tolerance of the SOFC to fuel contaminants such as Siloxanes and sulfur compounds [4,24], which are both commonly found in biogas, a deep removal stage for impurities is always required. Recent studies have proved that siloxanes, in particular, are highly detrimental for the SOFC Ni-anode so they must be removed fully prior feeding the gas to the fuel cell module [2,3].

The clean-up process includes moisture removal together with sulfur and Siloxanes removal on adsorption beds filled with impregnated activated carbons. A comprehensive review of biogas quality issues for integration with fuel cells is provided in Ref. [4].

2.3. SOFC system

Figure 3 illustrates the SOFC system layout operated in combined heat and power (CHP) mode. Three modules are considered for installing in the plant to avoid biogas shortage during the summer season when less biogas is available; hence, the three modules can operate at capacity factor close to the unit, while adding a fourth module would decrease the overall capacity factor of the SOFC installation significantly.

On the one side, cathode air is fed to the SOFC through a blower (outlet pressure from the blower is set at 1.31 bar to compensate the pressure loss within the system) and pre-heated in the air heat exchanger. Clean biogas, on the other hand, is also fed through a blower to the SOFC. Fuel gas is first mixed with the anode gas recycle to provide pre-heating of the fresh fuel as well as sufficient steam content to drive the following reforming reactions and avoid the use of external demineralized water (recirculation is controlled to maintain a fixed SC of 2 at the reformer inlet).

The mixed gas, found at around 450 °C, is fed to the pre-reformer where a fraction (~10%) of the overall methane is converted to the hydrogen through reforming and shifting reactions. The pre-reformer is modeled as an adiabatic reactor, where outlet temperature (420 °C) and methane conversion are calculated depending on the inlet conditions. No heat from external is thus required in this configuration [27,28].

Then, the pre-reformed gas is pre-heated through the fuel heat exchanger before feeding the anode side of the stack. The fuel gas experiences an internal reforming, which brings hydrogen-rich products to participate in the electrochemical reaction inside the fuel cell stack. Internal reforming has been considered as IIR (Indirect Internal Reforming), thus taking place inside the same insulated volume but on a separated catalyst (only thermally connected to the stack). The electrochemical reaction generates thermal energy, a part of which is used to deliver the required heat for the internal reforming reaction, another part is employed to heat up the cell products and the residual reactants. The anode and cathode exhaust gasses with higher

temperature are obtained, and electrical power is produced. An inverter is used to convert the DC power generated by the stack into AC grid-quality electricity.

After accomplishing the electrochemical reactions in the SOFC, the excess air exiting the cathode and a fraction of the unreacted fuel exiting the anode are supposed to combust completely in the after-burner. However, the other fraction of anode exit gas is recirculated back to the mixer to be mixed with fresh biogas fuel.

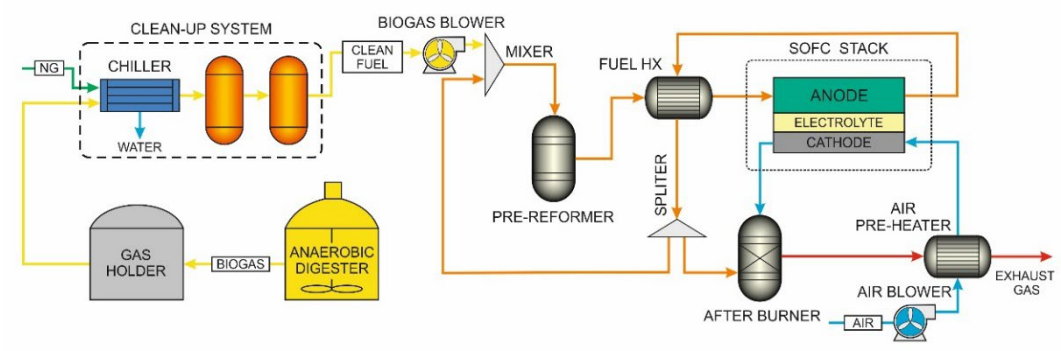

Figure 3: Clean-up unit and SOFC system layout.

2.4. Heat recovery configuration

In the current plant design, the produced biogas in the SMAT Collegno WWTP is burned in a boiler to supply the heat demand of the digester; however, in DEMOSOFC project, a significant amount of produced biogas will be fed into the SOFC units and consequently there will be a shortage of biogas to heat up the digester. The first possible way to supply that part of required heat is the utilization of the exhaust thermal energy of SOFC systems (first loop in Figure 4). When the recovered heat is not sufficient to supply entire amount of the digester thermal load, an auxiliary boiler fed by either extra biogas or natural gas (second loop in Figure 4) along with a concentrated solar power system (third loop in Figure 4) are used to provide the rest of the thermal load. In Italy, the mean annual solar radiation ranges from 3.6 kWh per square meter per day in the Po river plain area to 4.7 kWh per square meter per day in Central-Southern Italy, to 5.4 kWh per square meter per day in Sicily. Consequently, even if Southern regions

have a production potential that is very high, the entire national territory is characterized by very favorable conditions for the installation of plants for the production of solar power. The thermal energy produced from the solar source can be used in WWTP for supplying heat to the digester.

Figure 4 shows the system layouts for extracting waste heat from SOFC system during the generation of electrical power and thermal integration of the plant with two different configurations (Case 1 is the baseline plant without solar integration, Case 2 is related to the use of CST). Referring to Figure 4, the systems consist of the following subsystems: (1) three SOFC modules, (2) three exhaust heat recovery exchangers, (3) a main heat exchanger (4) an auxiliary boiler which is equipped with a burner, (5) concentrating solar power system (CST), (6) heat exchangers (7) pumps, (8) mixers, (9) splitters, and (10) anaerobic digester. The baseline plant and solar-assisted case are described in the following sections in detail.

2.4.1. Case 1 – Baseline plant

The exhaust gas exiting from three SOFC systems (streams 14a, 14b, and 14c) are used in three exhaust heat recovery exchangers (HX_a, HX_b and HX_c) to heat up the liquid water (stream 1). Then an intermediate closed loop (first loop) is embedded to deliver the recovered heat to a fraction of the sludge (stream 7) flowing to the anaerobic digester using a heat exchanger (HX1). When the recovered heat from the SOFC plant is not sufficient to heat up the total amount of sludge and meet the whole digester thermal load, an auxiliary boiler will be employed. Thus, to provide the required heat for the digestion process, some amount of natural gas/biogas (streams 9a and 9b) should be burned in the boiler. Second water loop is used to receive the heat from the boiler and transfer it to the second fraction of the sludge flow (stream 6) using a heat exchanger (HX2). In the end, a mixer is used to mix two sludge streams in a single stream, which is then fed into the anaerobic digester.

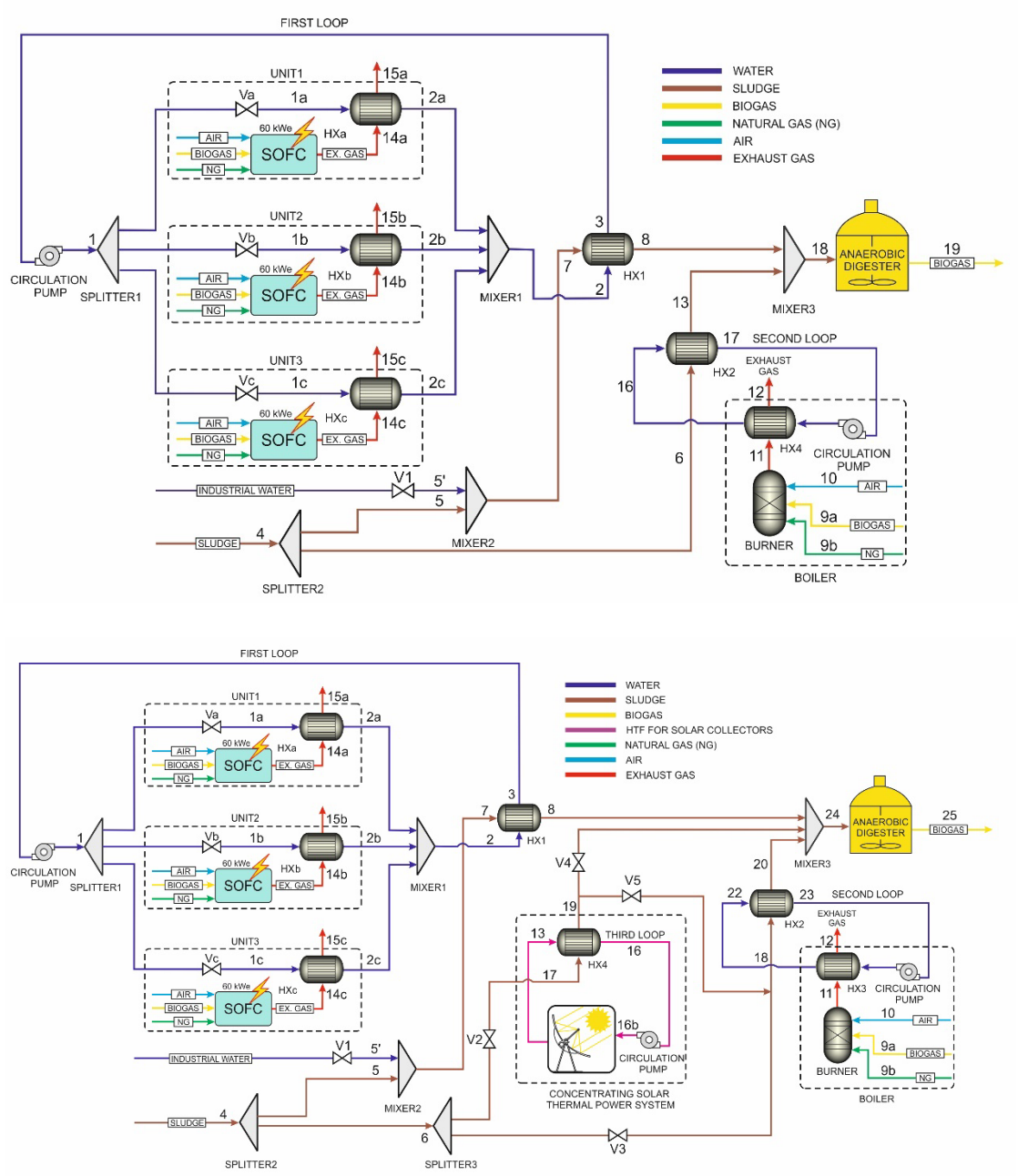

Figure 4. The layout of the heat recovery section of the plant. On the top: Baseline plant (Case 1). On the bottom: a concentrated solar thermal system in series/parallel with boiler (Case 2A/2B).

2.4.2. Case 2 – Solar-integrated plants

In the case of integration with solar collectors, two possible layouts (series and parallel) have been proposed. The difference is related to the connection between the CST system sludge heat-exchanger and the auxiliary boiler sludge heat-exchanger. In Case 2A the two components are connected in series, while in Case 2B they are connected in parallel. In the series mode,

sludge is first sent to the solar loop (third loop) to be warmed up by solar energy. Then the sludge with higher temperature goes to the boiler loop (second loop) where it is heated up to the determined temperature. Whereas, in the parallel mode, the sludge is split into two streams (streams 17 and 18). A part of sludge is sent to the solar loop while the rest goes to the boiler loop. To operate the systems under series and parallel modes the valves should be adjusted according to Table 2. It should be noted that for all the cases, the main part of sludge is heated up by the first loop (SOFC exhaust gas).

Case 2A: In this second layout, the sludge stream which is not connected to the SOFC exhaust first loop (sludge stream 6) is heated up using both thermal energies from CST system and boiler respectively. As mentioned earlier, the CST system is used to decrease the boiler fuel consumption. A heat exchanger (HX4) is employed to transfer thermal energy from the third loop to the sludge. Then the partially heated sludge by CST system is heated up to the required temperature using the auxiliary boiler (second loop).

Case 2B: The main difference with case 2A is to put the CST system and the boiler in a parallel way. For this purpose, another splitter is used to divide the sludge stream 6 into two streams (17 and 18). In this case, there are three streams, instead of the two original ones, that are mixed in the final mixer.

Table 2. Status of the valves for different operational modes.

Valve		V_a, V_b, and V_c	V1	V2	V3	V4	V5
Baseline plant (Case 1)		Open	Closed	-	-	-	-
Solar Integrated Plants	Case 2A	Open	Closed	Open	Closed	Closed	Open
	Case 2B	Open	Closed	Open	Open	Open	Closed

3. Mathematical modeling

In this section, the thermodynamic modeling of the proposed systems is going to be described.

3.1 Energy analysis

3.1.1 Assumptions applied to the current analysis

The following conceptually reasonable assumptions are made for the analysis:

- The atmospheric air is composed of 79% N_2 and 21% O_2, on a volume basis.
- The natural gas composition is assumed to be 100% CH_4.
- All gasses are treated as ideal gasses and gas leakages from the components, and the connecting pipes are negligible.
- The analysis is carried out under thermodynamic equilibrium and steady state conditions.
- Changes in kinetic and potential energies are neglected.
- Temperatures at channel inlets are the same and, similarly, temperatures at the channel exits are the same.
- Heat exchangers are insulated so that no heat interaction with the environment takes place.
- Unreacted gases are assumed to be fully oxidized in the afterburner of the SOFC system as well as the methane gas in the burner of the boiler.

The input data for systems' simulation are listed in Table 3.

Table 3. Input data for the SOFC system and plant components.

SOFC system		
	Single Cell active surface area	50.00 (cm^2)
	DC–AC inverter efficiency	96 (%)
	Fuel utilization factor	85.0 (%)
	Base inlet temperature to SOFC	800 (^oC)
	Number of cells	5’500 (-)
	Steam-to-carbon ratio	2 (-)
Heat Exchangers		
	Heat exchanger pressure drop	2-5 (%)

3.1.2 System modeling

The logical steps and workflow of the system modeling approach used in this work are illustrated in Figure 5. Referring to the flowchart, given the sludge mass flow rate reported by SMAT as well as set the temperature values for required state points, the thermal demand of digester can be calculated. On the other hand, fixed the number of fuel cells, their active surface

area, fuel utilization and current density, the molar flow rate of anodic gases and air at the inlet and outlet of the stack as well as the output electrical power and exhaust heat recovery are calculated. For the sake of brevity, the detailed assumptions, and equations used for the SOFC modeling are presented in Appendix.

Whenever the SOFC requires an amount of biogas that is more than the available one in the gas holder, natural gas from the grid is supplied in order to maintain the SOFC operating at full load. Otherwise, the amount of biogas which is not used for SOFC system is stored in the gas holder to burn in the boiler to provide thermal demand of digester. Considering the heat recovery potential from the SOFC system, the residual heat demand of digester can be calculated. If the thermal heat recovery from the SOFC system is more than the required thermal demand of digester, there will be no need to use a boiler or solar system. Otherwise, the remained heat demand of digester will be supplied using the solar system and the boiler. Given a proper guess value for the solar collector area, an amount of solar thermal energy can be calculated then the boiler will provide the rest. For the boiler modeling, if the excess biogas becomes enough for providing the required energy of the boiler the modeling will be completed otherwise some amount of natural gas from the grid will be burnt in the boiler. In the end, desirable output such as net electrical power, system efficiency overall amount of natural gas taken from the grid, contribution of solar system, boiler and SOFC system in providing the digester thermal demand are obtained.

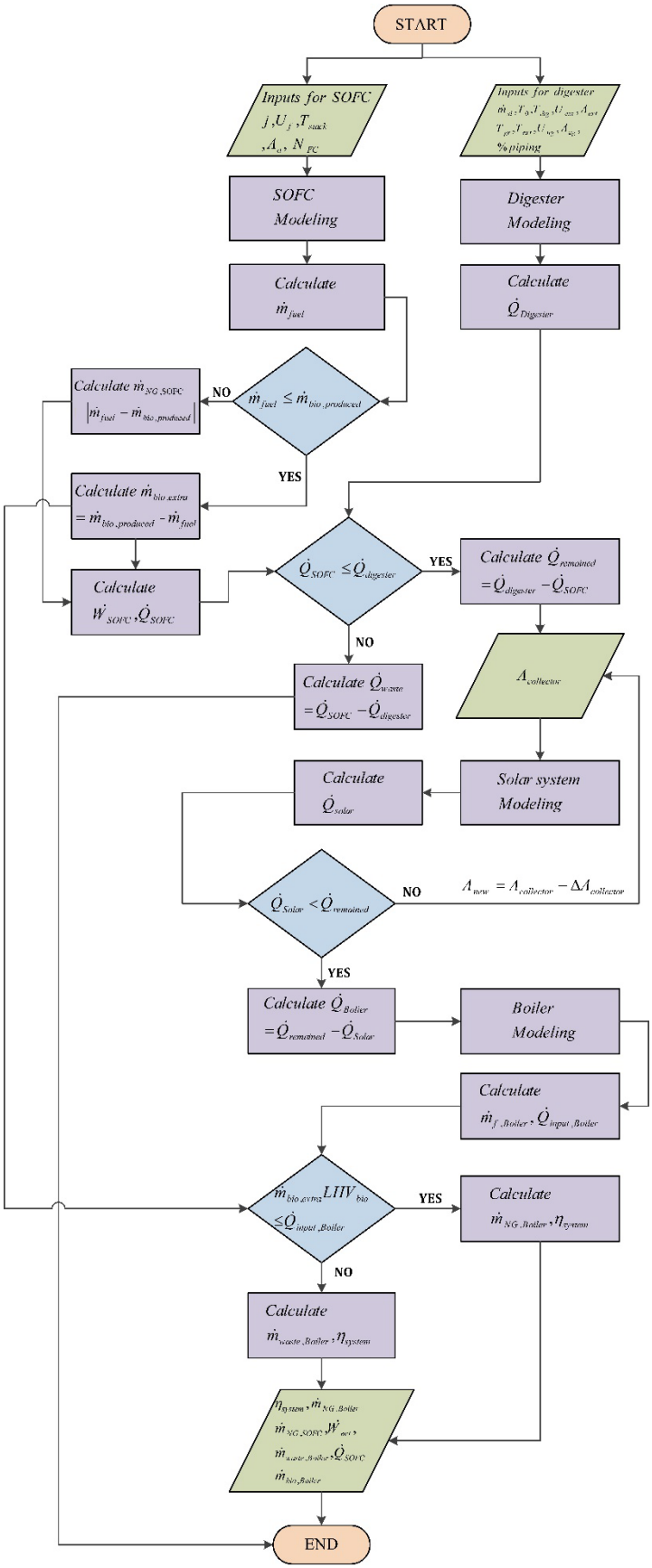

Figure 5 Logic steps of the modeling approach used for energy system analysis.

3.1.3. Concentrated solar thermal system (CST)

The considered collector would be the PTCs (parabolic trough collectors). It is made by a sheet of reflective material into a parabolic shape, where the beam irradiation incident is reflected into the receiver tube. The receiver tube is a black metal tube placed along the focal line of the receiver where working fluid is flowing through it. The PTC efficiency is not steady and is affect by the heat losses to environmental and the useful heat removed by working fluid. The heat losses at air side are determined by cover temperature, environmental temperature, and wind velocity.

The useful heat at working fluid side is determined by the temperature difference between work fluid and surface and flow configuration. To reduce the heat losses, an evacuated concentric glass tube (cover) is employed around the receiver. The collector *IND300*, one of the smaller models of Parabolic Trough Collectors (PTC) family is selected. The IND 300 PTC's efficiency is given as [29,30];

$$\eta_{IND300} = 0.733 - 0.238 \cdot \left(\frac{\bar{T}_{wf} - \bar{T}_0}{G}\right) - 0.0013 \cdot G \cdot \left(\frac{\bar{T}_{wf} - \bar{T}_0}{G}\right)^2 \quad (1)$$

Where, $\bar{T}_{wf}$ and G are the average collector working fluid temperature and direct (or beam) normal irradiance (BNI), respectively, and $\bar{T}_0$ is the ambient temperature. The beam and diffuse irradiances for the Turin city are available in [31] on a monthly basis.

3.1.4. Heat Recovery Unit

The heat recovery unit (HRU) has been modeled by knowing the heat available from the SOFC exhaust and the total digester heat demand.

The total digester thermal load (Q_{dig}), expressed in kW, is calculated on a monthly basis as the sum of the following contributions:

- the thermal power required for the sludge heating up: from a variable inlet temperature (14-23 °C depending on the season) to the digester temperature (38-47 °C, taken from real WWTP measurements), Q_{sl};
- the heat losses through the digester walls, Q_{los};
- the heat losses through piping, Q_{pipes}

Finally:

$$Q_{dig} = Q_{sl} + Q_{los} + Q_{pipes} \quad (2)$$

The first term in (Eq. 2) is calculated based on:

- the sludge mass flows rate $\dot{m}_{sl}$ (the average monthly value is used as calculated from the SMAT hourly measurements);
- the sludge inlet temperature $T_{sl,in}$ (taken from a WWTP in Nosedo (Milan, IT) [32,33])
- the digester constant temperature T_{dig} (calculates as average value from SMAT hourly measurement);
- since the solid content in sludge lower than 2% (weight), the specific heat capacity is calculated, c_p, is taken as equal to that of water.

The sludge pre-heating term is written as:

$$Q_{sl} = \dot{m}_{sl} \cdot c_p \cdot \left(T_{dig} - T_{sl,in}\right) \quad (3)$$

The digester thermal losses have been evaluated using (Eq. 4):

$$Q_{los} = Q_{ug} + Q_{ext} \quad (4)$$

Where:

$$Q_{ug} = U_{ug} \cdot A_{ug} \cdot \left(T_{dig} - T_{gr}\right) \quad (5)$$

$$Q_{ext} = U_{ext} \cdot A_{ext} \cdot \left(T_{dig} - T_{ext}\right) \quad (6)$$

$Q_{ug}$is the term for losses through the underground surface (heat exchange between walls and ground). Q_{ext} accounts instead for losses through the external surface (heat exchange between walls and external air).

Finally, the thermal losses through the piping have been evaluated as a fixed share ($\%_{pipes}$) of the total sludge pre-heating duty and digester thermal loads (Eq.7):

$$Q_{pipes} = \%_{pipes} \cdot (Q_{sl} + Q_{los}) \quad (7)$$

Explanation and values used for calculating the thermal terms are given in Table 4.

Table 4. Main parameters for digester thermal load calculations.

Parameter	Symbol	Value	Unit	Ref.
Sludge inlet temperature	$T_{sl,in}$	14 (January) ÷ 23 (July)	°C	Nosedo WWTP
Digester temperature	T_{dig}	42.14 °C (average yearly value)	°C	SMAT
Sludge mass flow rate	$\dot{m}_{sl}$	1.82 (December) ÷ 3.09 (May)	kg/s	SMAT
Heat transfer coefficient for underground walls	U_{ug}	2.326	W/m^2°C	SMAT
Heat transfer coefficient for non-underground walls	U_{ext}	0.930	W/m^2°C	SMAT
Area of underground walls (floor and partial side walls)	A_{ug}	450.8	m^2	SMAT
Area of non-underground walls (partial side walls and roof)	A_{ext}	1132.1	m^2	SMAT
Ground temperature	T_{gr}	5 (winter) ÷ 10 (summer)	°C	HP
External temperature	T_{ext}	2.3 (February) ÷ 23.9 (July)	°C	ilmeteo.it
Percentage of losses through pipes	$\%_{pipes}$	5	%	HP

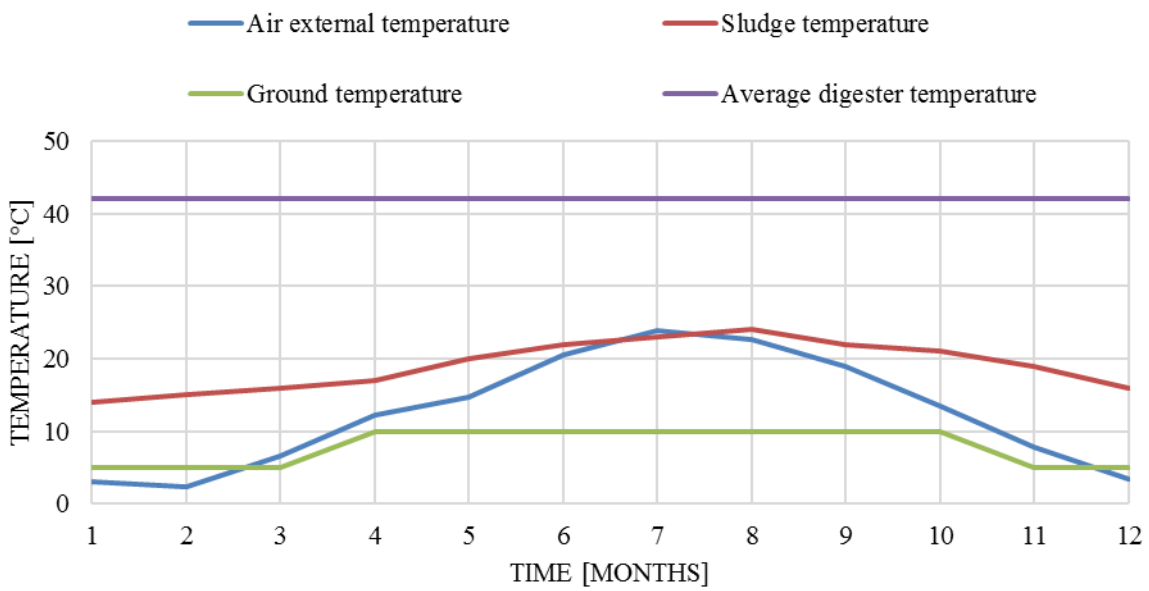

Figure 6. Digester, sludge inlet, air and ground temperature trend.

The total digester thermal load values and trend are shown in Figure 6. The digester thermal load will be covered partially by the SOFC heat recovery system and partially by the boiler and solar system. The boiler will be fed first with extra-biogas and then with NG from the grid.

The heat exchangers have been designed to work at fixed temperatures and variable flow rate in case of off-design conditions. $HX_{a,b,c}$ and HX1 have been designed based on the SOFC nominal thermal production, HX2 based on a month with the highest boiler thermal load (January) and HX4 based on a month with the highest solar production (July). The operational temperature for each heat exchanger is shown in Table 5.

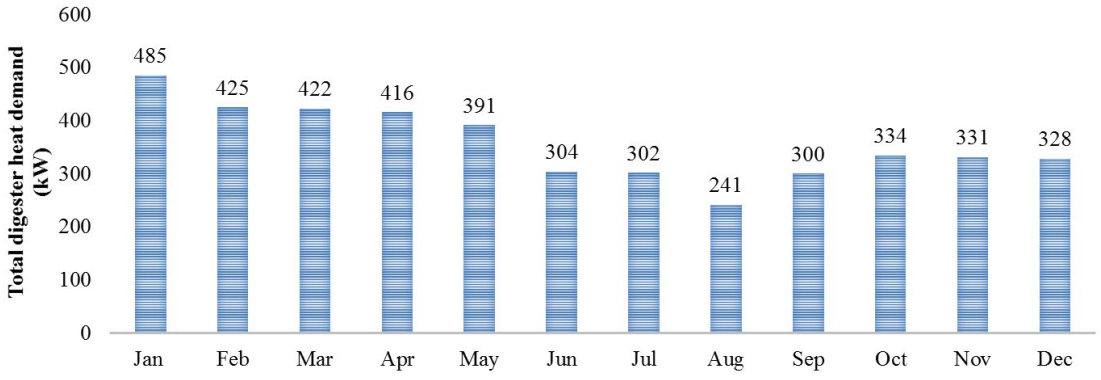

Figure 7. Total digester heat demand, including sludge pre-heating and digester thermal losses.

Table 5. HRU temperatures.

		Temperature IN - °C	Temperature OUT - °C
$HX_{a,b,c}$	Hot side – Exhaust gas	279.2	70
	Cold side – Water	42	78
HX1	Hot side – Water	78	42
	Cold side – Sludge	14 (January)	52.66 (January)
HX2	Hot side – Water from boiler	70	35
	Cold side – Sludge	14 (January)	52.66 (January)
HX4	Hot side – Water from solar	100	40
	Cold side – water	23 (July)	50.41 (July)

3.3. Economic analysis

The economic analysis has been performed to evaluate the economic performance of the various system configurations. The economic evaluation has been performed for the entire system control volume, spanning from the clean-up system to heat recovery unit including the solar system. Different case studies and sensitivities analyses are also presented to evaluate the influence of the system parameters on the final economic results.

The analysis has been performed by calculating sequentially:

- Investment costs (CAPEX)
- Operation costs and earnings evaluation (OPEX)
- Cash-flow analysis and LCOE evaluation

Capital costs refer to the following four plant sections:

- Clean-up unit (CU)
- SOFC module (SOFC)
- Heat Recovery Unit (HRU)
- Concentration solar system (CST)

3.3.1 Investment cost evaluation

The overall investment expenditure by the plant owner during the first year of a lifetime has been calculated. A 1-year installation period is assumed considering that several plant sections include turnkey equipment. Cost functions, reference and input data for the plant costing are given in Table 6.

Table 6. Investment cost equations.

	Item	Cost equation	Ref.
CU	Clean-up unit	Current scenario: 1000 \$/$kW_{AC,SOFC}$ Near term scenario: 500 \$/$kW_{AC,SOFC}$ Long Term scenario: 200 \$/$kW_{AC,SOFC}$	[28]
SOFC	Air and biogas blowers	Type: Centrifugal radial blower Material: SS	[29]
	Air and biogas pre-heaters	Type: Double pipe HX Material: Ni-NI U value: 50 W/m^{2}K	[29]
	Pre-reformer	% reforming ~ 10% Type: horizontal process vessel Material: Ni	[30]
	SOFC stack	$c_{stack} = 2130.2 \cdot PrV^{-0.404}$ Fitted equation	[31]
	After burner	$c_{AB} = \left(\frac{46.08\ \dot{m}_{ex}}{0.995-\frac{p_{out}}{p_{in}}}\right)[1 + e^{0.018T_{AB}}]$	[32][33]
	Inverter	$c_{inv} = 10^5 \left(\frac{W_{SOFC,DC}}{500}\right)$	[32][34]
	Piping	5% of SOFC module cost	HP
HRU	HXa,b,c Gas-water	Aspen Heat Exchanger Design & Rating® Comparison with Turton book (Double pipe, SS)	[29]
	HX1 Water/glycol – sludge HX2 Boiler water/sludge HX4 Solar water/sludge	Type: Double pipe Material: CS	[29]
	Pumps (main loop, boiler loop, solar loop)	Type: Reciprocating pump Material: CS	[29]
CSP	Solar concentrators	270 \$/m^2	[35]

3.3.2 Operation costs and revenues evaluation

From the second year of operation, the plant owner operational costs and electricity revenues are accounted in the cash-flow analysis. In particular, since the Italian subsidies on electrical production from sewage biogas are issued only for the electricity sold to the grid and are lower than the electricity cost [34], it has been assumed to have only self-consumption of the power

produced being the most convenient scenario. The SOFC system will be able to supply around 25-30% of the WWTP electrical needs.

As resumed in Table 7, operation costs are related to:

- Maintenance on clean-up unit (adsorption material substitution, chiller maintenance)
- SOFC stack substitution (with an assumed near term target lifetime of 6 years)
- HRU maintenance (cleaning of piping and HX)
- Solar system general maintenance
- Labor (assumed as 1 technical operator working 50% of his/her time on the plant)
- NG to the boiler. NG consumption is required for thermal load supply in case the SOFC heat recovery is not enough.

Other assumed input parameters for the economic analysis are also summarized below:

- Capacity factor: 95.7% from optimization analysis on the plant layout
- Electricity price: 0.16 €/kWh from SMAT Collegno WWTP
- NG price: 0.6 €/S m^3 from SMAT Collegno WWTP
- Depreciation rate: 10 % [35]
- Depreciation time: 10 y [35]
- Discount rate: 3%
- Tax rate: 30% for Italy [36]
- Plant lifetime: 20 y

The cash-flow analysis is used to evaluate the overall economic profitability of the system. Further details on the economic calculation methodology could be found in our previous work [35].

The Levelized Cost of Electricity (LCOE) has been calculated according to Ref. [37], and the equation is provided below:

$$LCOE = \frac{c_{inv} + \sum_{y=0}^{N} \frac{c_{op,y}}{(1+i)^y}}{\sum_{y=0}^{N} \frac{W_{el,y}}{(1+i)^y}} \quad (8)$$

Table 7. Operating cost equations.

	Item	Cost equation	Ref.
CU	Clean-up unit	Current: 2 c\$/kWh_{el}/y Near Term scenario: 1 c\$/kWh_{el}/y Long Term scenario: 0.5 c\$/kWh_{el}/y	[28]
SOFC	SOFC stack substitution	c_{stack}/6y Lifetime 6 y	[31]
HRU	HRU and plant general maintenance	2% of total plant investment cost	HP
CSP	Concentrators	5% of CSP investment cost	[40]
	Labor cost	1 operator working 50% on the installation	[41]
	NG to boiler	Calculated depending on the digester thermal load and the SOFC heat recovery production	

3.4. Energy efficiency

Energy efficiency for the overall system can be defined as:

$$\eta_I = \frac{\dot{W}_{net} + \dot{Q}_{recovery}}{\left(\dot{m}_{biogas} \cdot LHV_{biogas}\right)_{SOFC} + \left(\dot{m}_{NG} \cdot LHV_{NG}\right)_{boiler}} \quad (9)$$

Where $\dot{W}_{net}$ is the net output power (stack AC power minus the blowers and pumps power consumptions) and $\dot{Q}_{recovery}$ is the total heat recovered. In the denominator, there is the sum of the biogas consumption for the SOFC system, the NG consumption for the boiler.

5. Results and discussion

5.1 Energy analysis

Results of SOFC modeling for the nominal condition are presented in Table 8. It is calculated that at the nominal condition, each SOFC module can produce a net electrical output power of 60kW but also 43kW of thermal energy from its exhaust gas could be achieved.

Operating conditions and performance of the fuel cell at full load are presented in Table 8.

Table 8. Operating condition under nominal load.

Load	Nominal	Unit
Current density	3781	A/m^2
Current	18.91	A
Cell voltage	0.6577	V
Fuel inlet flow	20.78	kg/h
Anode recycle ratio	0.557	-
Exhaust temperature	279.2	°C
Exhaust mass flow rate	0.1992	kg/s
Stack AC power	65.6	kW
Air blower power	5.268	kW
Fuel blower power	0.181	kW
Thermal load	42.37	kW
Electrical efficiency	51.62	%
Total efficiency	87.98	%

Thanks to the hourly volumetric flow rate of sludge as well as the amount of biogas production reported by SMAT (Figure 8), the monthly average volumetric flow rate of sludge and biogas production have been calculated.

The biogas analyzed in this work is produced from the anaerobic digestion of sludge, which is collected from the treatment of mixed urban/industrial wastewater. (We have used real data for the WWTP serving a fraction of the city of Torino, ITALY). During the summer season, less wastewater is collected since there is a reduction in urban population (due to holidays). Also, the industrial activity decreases (especially during August). The overall effect is a lower organic load entering the plant, and thus less biogas is produced.

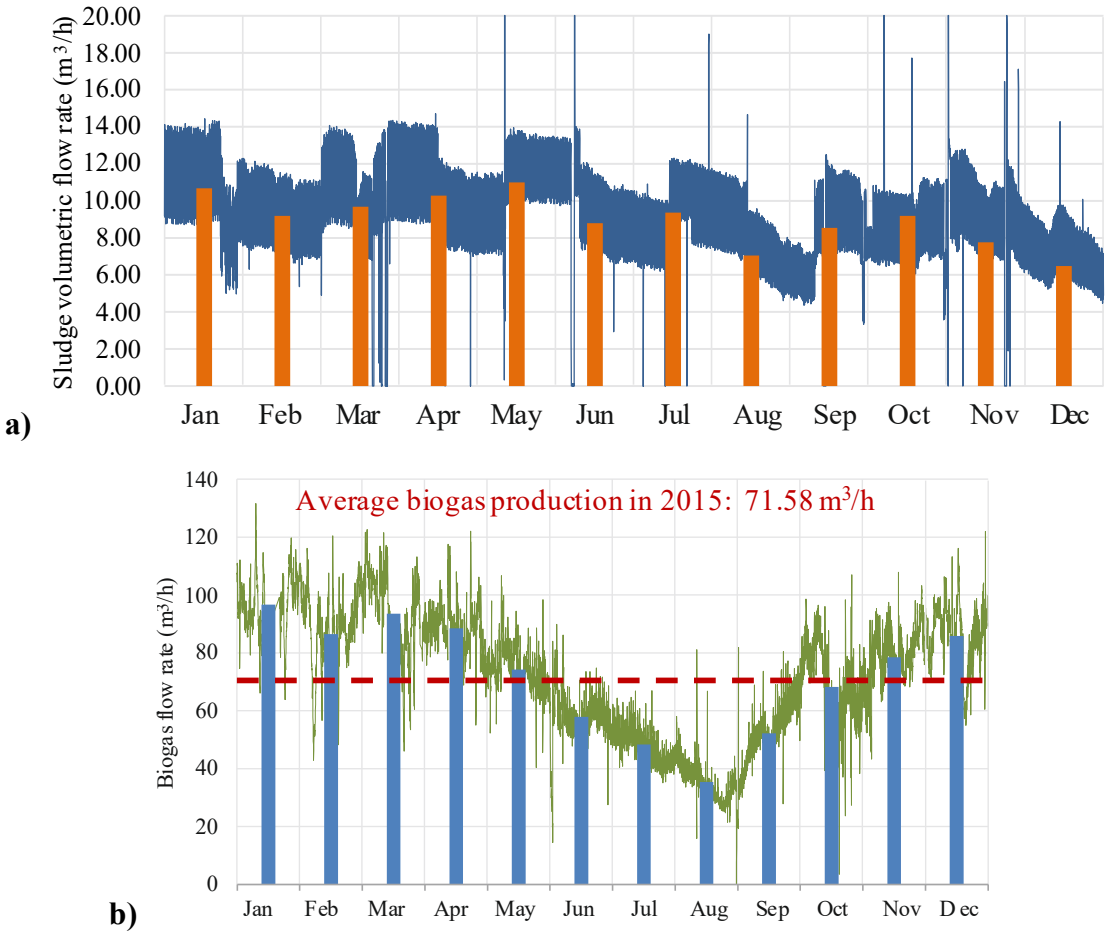

Figure 8: a) Hourly and monthly volumetric flow rate of sludge treated in the anaerobic digester and, b) Biogas production.

As shown in Figure 8, for the base case, using the sludge volumetric flow rate as an input, the NG consumption in the boiler is obtained to keep the digester at the required temperature. For the solar-integrated case, the results of NG consumption for providing 25%, 50%, and 75 % of boiler thermal energy are also presented in Figure 8. The results confirm that increasing the solar contribution from 25% to 75% has a remarkable impact on NG consumption. It can be seen that when 50% of boiler thermal load is compensated by the solar system, there is no need to bring in the NG from the grid for at least six months. This is because as burning the remained biogas in the boiler could provide most of digester heat demand, the need for supplying the NG to boiler will not be required with an increase in the solar contribution.

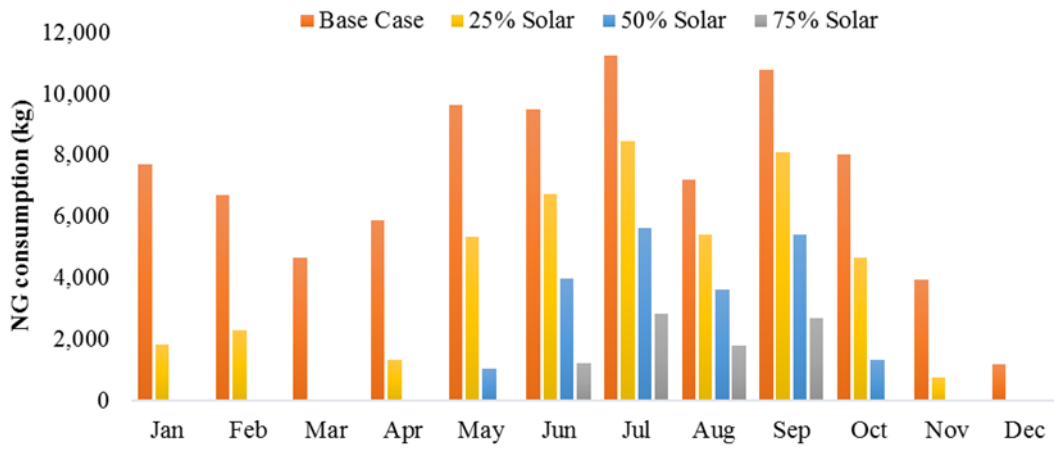

Figure 9: NG consumption for base case (without solar collectors) and solar cases with different contribution

Based on the calculations, it is found that for providing 25%, 50% and 75% of boiler heat using the solar system, 455 m^2, 910 m^2 and 1365 m^2 collector will be respectively needed based on six months average. To do a reasonable parametric study considering the available space for installing the solar collectors in the plant, collector sizing of 300 m^2, 500 m^2, 700 m^2, 900 m^2, and 1100 m^2 are selected (Figure 9). Referring to Figure 9, it is calculated that for the base case 39%, 29% and 32% of total digester demand are provided by SOFC exhaust heat recovery, burning biogas in the boiler and using external NG from the grid respectively. However, installing 300 m^2, 500 m^2, 700 m^2, 900 m^2, and 1100 m^2 solar collector results in increasing the solar contribution from 8% to 13%, 18%, 23% and 29% respectively. It can be observed that increasing the solar collector area will lead to a remarkable reduction in NG contribution for the digester thermal loads. For instance, when 1100 m^2 of solar collector is used the solar energy will cover 49 % of the total thermal energy of the boiler so that only 4% of contribution will be of using external NG from the grid.

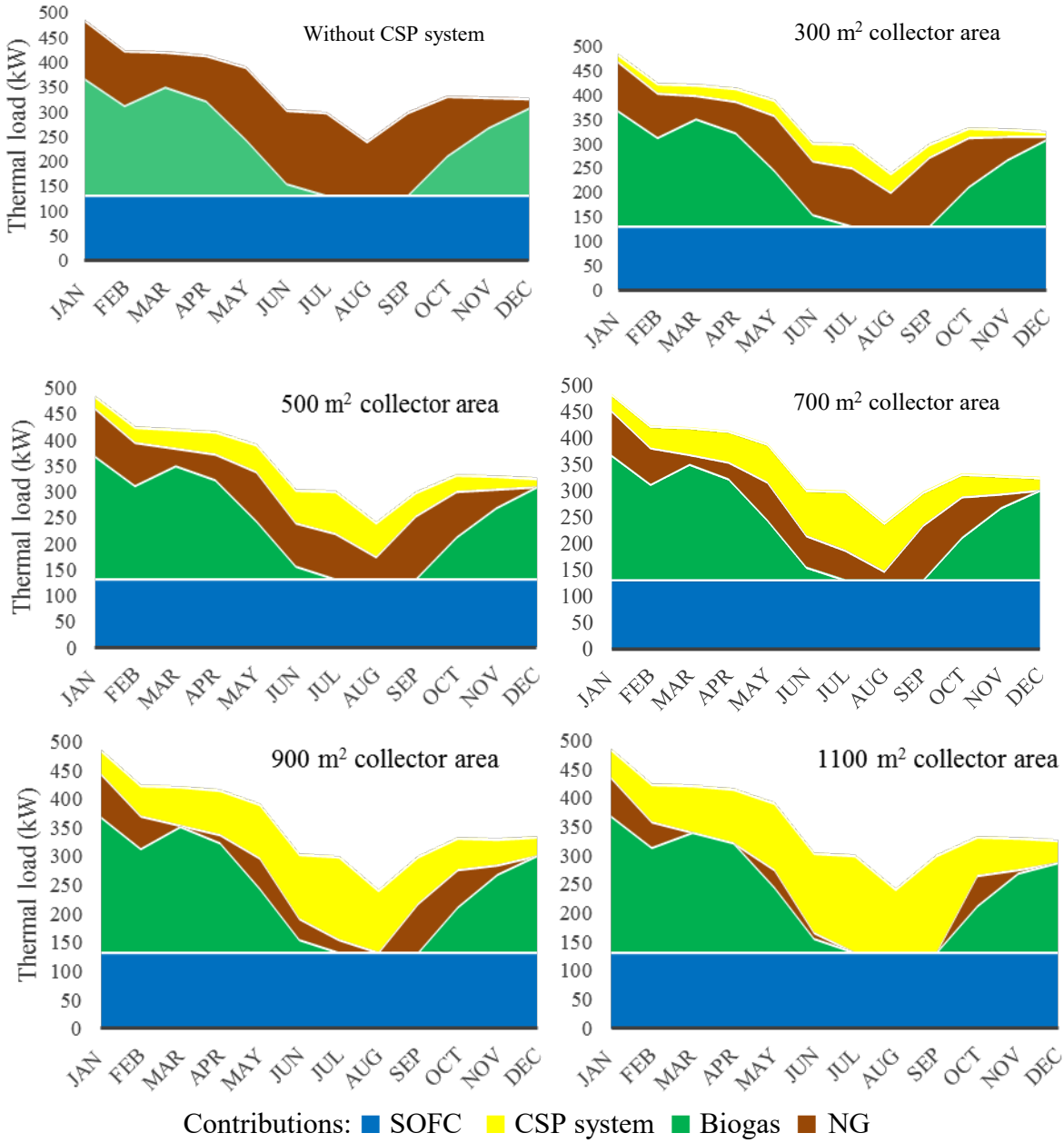

Figure 10. Thermal load maps with different solar collector areas.

Tabulated data related to the cases with 300 m^2 and 1100 m^2 area of the solar collectors are shown in Table 9. The first table shows that when 300 m^2 of CST system is utilized there will be no flaring of the biogas, whereas when 1100 m^2 of CST system is used 3%, 1%, and 7% of the produced biogas will be flared in March, April, and December, respectively. The reason for biogas flaring is due to the oversizing of the CST system in the large solar installation scenario: during some months the solar thermal production, together with the SOFC heat recovery, fully

cover the required digester thermal load, so extra-biogas (which normally would go to boiler) is flared (Noted that in this case NG consumption is also zero).

The amount of the annual NG reduction due to the contribution of the CST system in thermal energy production is depicted in Figure 10. As it can be seen in this figure even if 300 m^2 is utilized there will be 23.2% saving in annual NG consumption. The annual saving of 84.1 % can be achieved if 1100 m^2 of CST system is used.

Table 9. Monthly coverages of thermal energy in the WWTP cases with 300 m^2 (upper table) and 1100 m^2 (lower table) of the solar collector.

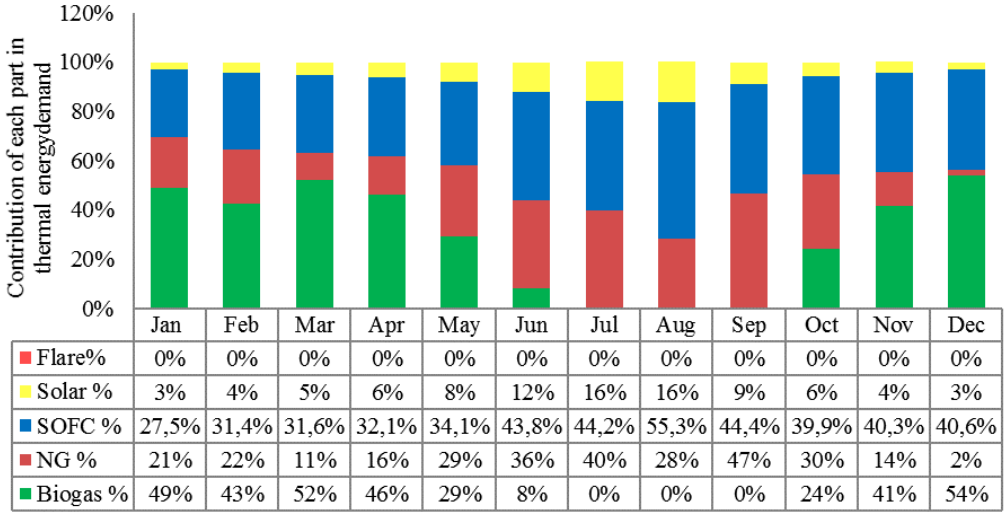

	Jan	Feb	Mar	Apr	May	Jun	Jul	Aug	Sep	Oct	Nov	Dec
Flare%	0%	0%	0%	0%	0%	0%	0%	0%	0%	0%	0%	0%
Solar %	3%	4%	5%	6%	8%	12%	16%	16%	9%	6%	4%	3%
SOFC %	27,5%	31,4%	31,6%	32,1%	34,1%	43,8%	44,2%	55,3%	44,4%	39,9%	40,3%	40,6%
NG %	21%	22%	11%	16%	29%	36%	40%	28%	47%	30%	14%	2%
Biogas %	49%	43%	52%	46%	29%	8%	0%	0%	0%	24%	41%	54%

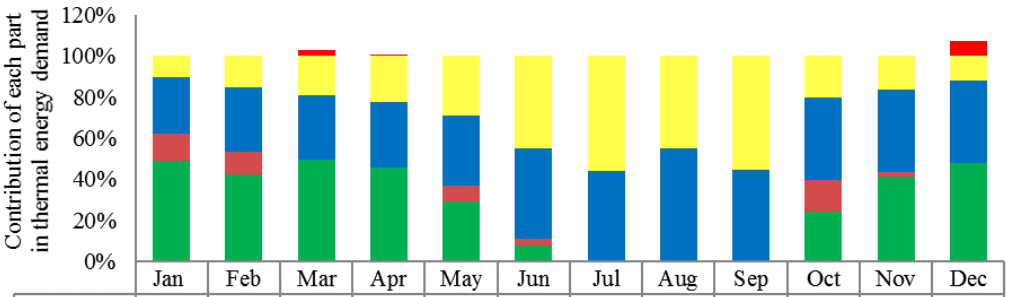

	Jan	Feb	Mar	Apr	May	Jun	Jul	Aug	Sep	Oct	Nov	Dec
flare%	0%	0%	3%	1%	0%	0%	0%	0%	0%	0%	0%	7%
Solar %	10%	15%	19%	22%	29%	45%	56%	45%	56%	20%	16%	12%
SOFC %	27,5%	31,4%	31,6%	32,1%	34,1%	43,8%	44,2%	55,3%	44,4%	39,9%	40,3%	40,6%
NG %	14%	11%	0%	0%	8%	3%	0%	0%	0%	15%	2%	0%
Biogas %	49%	43%	49%	46%	29%	8%	0%	0%	0%	24%	41%	48%

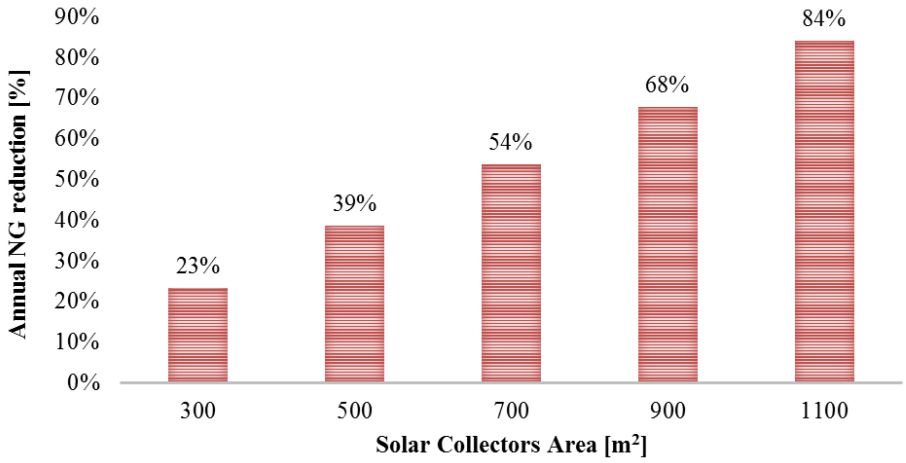

Figure 11. Reduction in natural gas consumption respect to base case.

5.2 Efficiency analysis results

The results of energy efficiency for the studied systems are shown in Figure 11. For case 1 the maximum and minimum energy efficiencies are found 66.33% in August and 41.27% in January respectively (this is due to the different monthly thermal load of the digester, which is higher in the colder months). However, as the results reveal, the solar case has higher system efficiency because methane consumption in this case decreases. The maximum efficiency enhancement of 11.8% is obtained for the July.

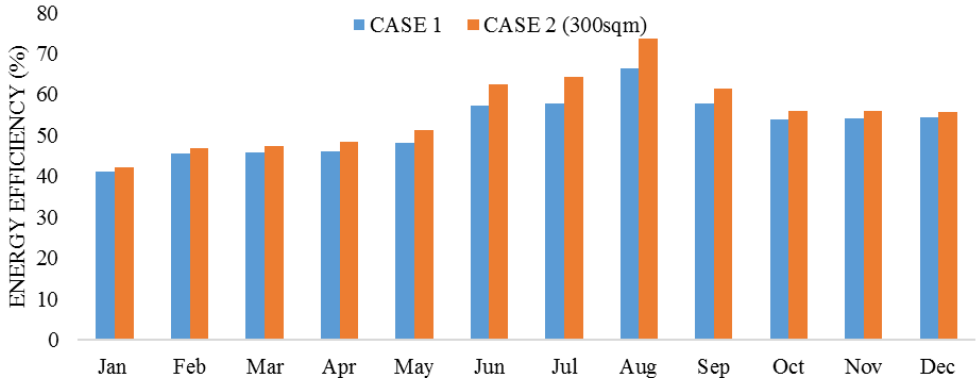

Figure 12 Energy efficiency for the base case (1) and solar case (2) scenarios.

5.3 Heat Recovery unit design

The heat recovery system has been first modeled in AspenPlus® to identify the flow rates in the different scenarios, and then has been sized using the Aspen Exchanger Design and Rating,

which provides a completely mechanical, thermal and economic definition of the heat-exchangers. The design has been made for all the heat-exchangers, using the Shell-and-Tube design. Results will be presented for the exhaust gas – water HX.

Input data for the system are the exhaust stream temperature, composition and flow and the desired temperature change on the water side. Chosen material is 316L because it can tolerate high temperatures. Fouling resistance has been set to zero as an assumption. The hot fluid has been supposed on the tube side. Results regarding dimensions, heat, exchanged and costs are summarized in Table 10 and Figure 12. The layout was achieved by fixing the maximum HX diameter according to SOFC module manufacturer specifications on available space inside the module for the DEMOSOFC project.

Table 10. Gas-water heat-exchanger main results.

Shell ID	mm	250.82
Tube length - actual	mm	3048
Tube length - required	mm	2571.2
Pressure drop, SS	bar	0.02004
Pressure drop, TS	bar	0.02066
Baffle spacing	mm	250
Number of baffles		10
Tube passes		1
Tube number		81
Total price	€	12’814
Area Ratio (dirty)	*	1.19
Film coefficient. overall, SS	W/m^2K	822.2
Film coefficient. overall, TS	W/m^2K	45.2
Heat load	kW	46.1

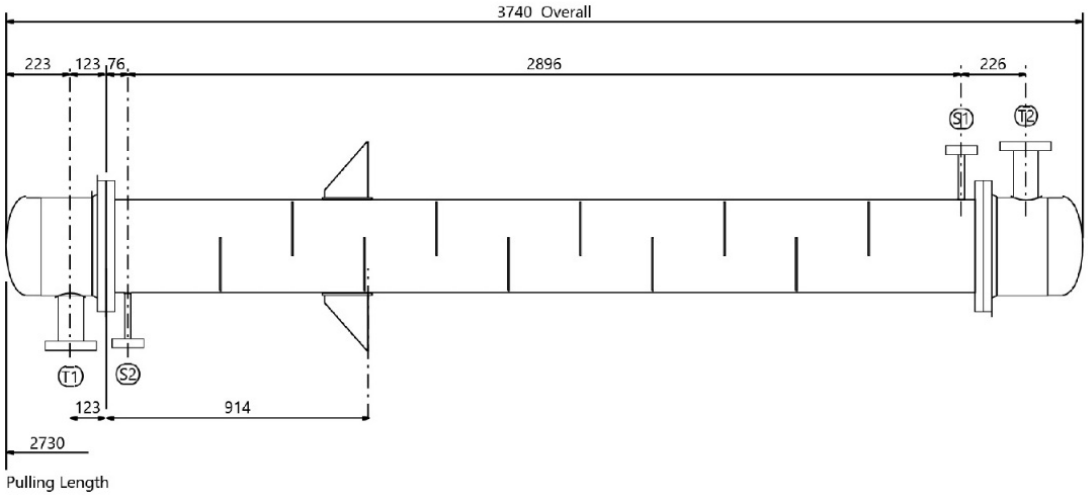

Figure 13. Gas-water heat-exchanger design.

5.4. Economic results

The economic analysis has been performed for the base case '1' and for cases '2A' and '2B' (these are the plant configurations that include solar collectors, having the boiler and solar contributions either in parallel or series).

Target costs for both SOFC and clean-up systems have been used. Both systems are expected to experience a fast technology learning in the coming years as more installation are deployed. In Figure 13 the expected technology learning for both OPEX AND CAPEX of the clean-up systems are shown. Base case analysis is performed with near-term costs (as for the SOFC unit).

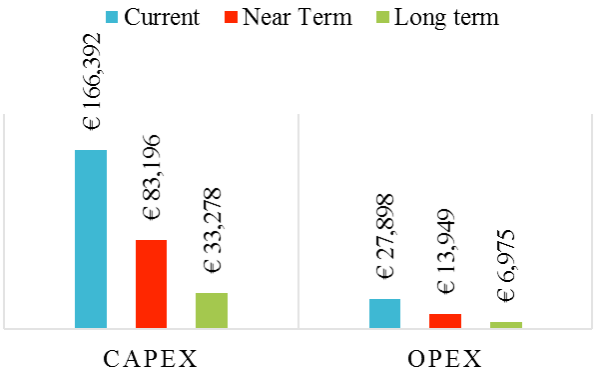

Figure 14. Clean-up system cost [38].

The target SOFC cost used in this work refers to an annual production volumes of 1 MW/y (which correspond to ~ 2,000 €/kW for the stack only), according to [39]. This value was calculated by fitting the SOFC capital cost trend shown in Figure 14 for the 1 MW/yr production (near-term scenario). The SOFC stack cost is also confirmed by a 2015 study from Roland Berger [40], in which a similar cost is reported for the 50 kWe SOFC module and a cumulative production of 1,000 units (50 MW). Furthermore, a sensitivity analysis has been performed on this value to show the impact of production volumes on the whole plant economic performance.

Starting from the SOFC stack, the Balance of Plant (BoP) components have been taken into account as detailed in the methodology section, and SOFC module cost breakdown is presented in Table 11. The overall module cost is around 3,000 €/kWe and the BoP thus accounts for ~1,000 €/kWe.

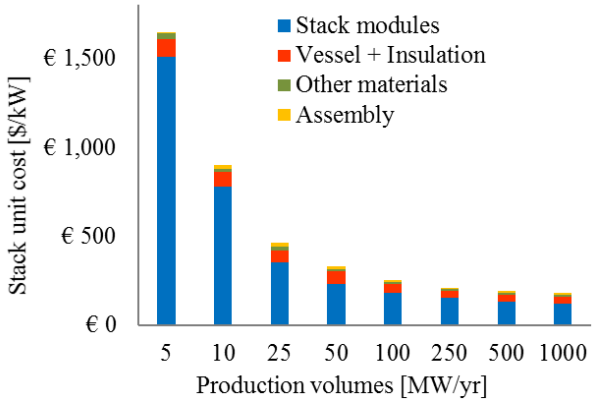

Figure 15. SOFC stack cost. [39]

Table 11. SOFC Modules Cost Breakdown.

Component	Cost [€]	Share [%]
Biogas blower	1,300	0.22%
Biogas pre-heater	22,105	3.69%
Reformer	32,785	5.48%
Air blower	7,890	1.32%
Air pre-heater	31,944	5.34%
SOFC stack	424,126	70.84%
After-burner	152	0.03%

Inverter/ Electronics	37,411	6.25%
Piping	41,030	6.85%
SOFC module cost	598,743	
SOFC specific module cost	**3,042**	**€/kW**

For what concerning the HRU, as shown in Figure 15, the only difference among cases 2A and 2B is the HX2 and HX4 cost, since flow rates and temperatures change as depending on the series/parallel configuration. Heat-exchanger costs have been calculated both using the Aspen Exchanger Design & Rating® and cost functions provided in the Turton hanbook [41]. Results are in the same order of magnitude between the two sources (max. difference is about 20-30% depending on the material). Since the Turton handbook was the reference providing higher costs, it has been adopted for the HX1, HX2 and HX4 (to perform a precautionary analysis), while the Aspen Exchanger Design & Rating® software has been used for the gas-water HXa, HXb and HXc cost (since here the difference with Turton book is lower than 10%). The difference regarding HRU cost between plants 2A and 2B is shown in Figure 15 together with results for the base case. Cases 2A and 2B show an increase, respect to case 1, of 15% and 17% respectively regarding HRU costs. Furthermore, in case 2B, a reduction in HX4 cost can be seen respect to case 2A, which leads to a total HRU cost of 79'465 € instead of 80'978 € (~2% reduction). Because of the non-impacting difference among cases 2A and 2B, the economic analysis will be presented only for case 2B, where the parallel configuration is chosen.

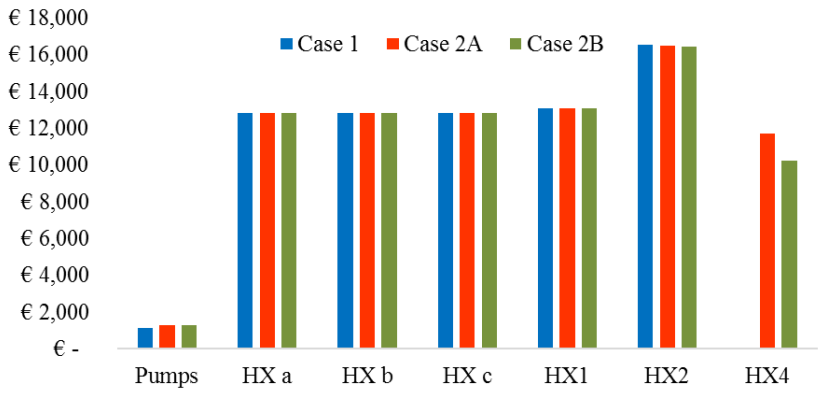

Figure 16. HRU cost.

The total investment cost has been determined and is reported in Figure 16 for the base case (1) and solar scenario (2B). The increase in costs (+ 12%) of the second case is due to the cost for the solar system and the slightly higher HRU cost.

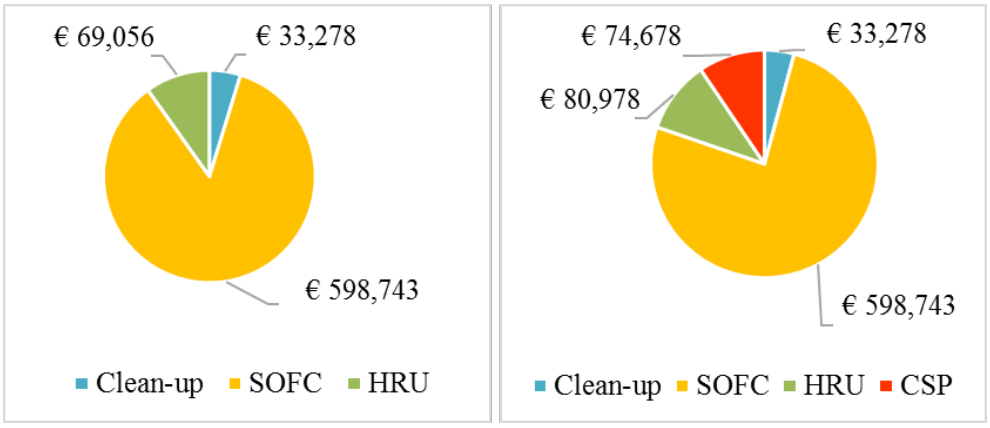

Figure 17. Total investment cost for case 1 (no solar, on the left) and case 2B (solar, on the right).

The second part of the economic analysis is related to operating costs. The higher investment cost of the solar scenario is offset by larger savings that derive from lower NG consumption, as explained before. As described in Figure 17, the increase in the HRU maintenance costs and the solar maintenance are compensated by the reduction in NG costs (-23%), showing advantages of the solar scenario from the operation point of view (total yearly operating cost is reduced by 8%). The positive economic performance of the solar system is shown in Figure 18: the cash-flow analysis shows that the payback time of the isolated solar concentration system is less than 9 years.

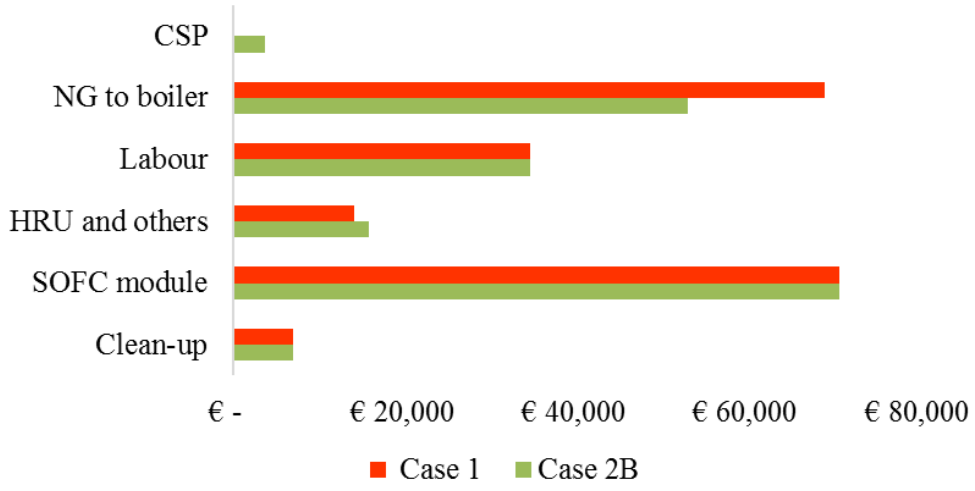

Figure 18. Operation cost is sharing in case 1 and 2B. SOFC module yearly cost has been calculated even if stack substitution occurs every 6 years.

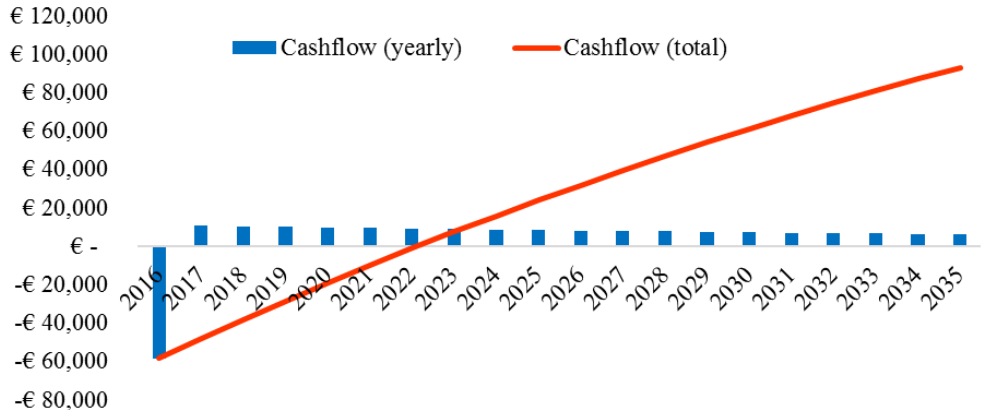

Figure 19. Cash-flow analysis of the solar concentration system.

Despite the positive economic profile of the CST system, because of the high SOFC investment cost and stack short lifetime, the cash flow of the total plant (Figure 19) shows a Pay Back Time (PBT) comparable with the system lifetime and thus a negative evaluation of the investment. The trend reductions in the net incomes every 6 years are due to the SOFC stack substitution, which covers more than 70% of the SOFC module costs and 47-52% of the total plant cost depending on the case study. The change on the curve slop after 10 years of operation is due to the tax increase because of the depreciation time conclusion (see [35] for more details on depreciation calculation methodology).

Figure 20. Economic evaluation for case 1 (no solar) and 2B (solar).

To analyze the effect of the main cost parameter (SOFC module) and the solar collector influence, different sensitivities analyses have been performed. In Table 13 the effect of increasing the solar collector area is presented. The specific cost has been reduced to the increasing area: 20% cost reduction for the 700 m^2 case and 40% for the 1100 m^2. The increase in the installed solar area, coupled with a cost reduction, is beneficial for the plant and points out the benefits of the solar respect to the base case. In particular, the PBT is reduced from 20 to 9 years among the base case and the 1100 m^2.

The LCOE is also shown in Table 13. For all the case studies, the LCOE is lower than the grid electricity price and, with increasing solar integration, the value is further reduced. Hence, the LCOE shows that, despite the long PBT of the investment, the electricity production during the entire system lifetime is competitive against grid electricity prices. Therefore, the solar installation entails a positive effect on the cost of the produced electricity.

Table 12. Sensitivity analysis on CST area, SOFC module and clean-up costs.

Installed CSP area [m^2]	PBT [y]	NPV @ end of life [€]
0	20	77,712
300	19	131,435
700	13.5	252,057
1100	9	446,055
SOFC annual production volumes [MW/yr]		

0.5	> lifetime	- 360,537
1	20	77,712
2	7.5	408,923
5	3.5	726,011
10	3	898,881
Clean-up cost [Scenario]		
Current	> lifetime	246,282
Near Term	20	77,712
Short Term	18	128,634

Table 13. Levelized Cost of Electricity.

Case study	**Energy Efficiency [%]**	**LCOE [€/kWh]**
Electricity from the grid price	---	0.16
Case 1 (no solar)	52.4	0.144
Case 2B (solar, 300 m^2)	51.9	0.141
Case solar 700 m^2	51.2	0.134
Case solar 1100 m^2	50.8	0.123

Despite the economic advantages of having a larger solar area, it is reasonable to consider, for the SMAT Collegno WWTP shown in Figure 1, to have a maximum installed area of 500-700 m^2 with a related PBT of 13.5 years.

The second analyzed variation is related to the clean-up unit cost. The sensitivity has been performed in the base case (case 1). The requirement of a clean fuel for feeding the fuel cell is currently converted in a high investment cost for the clean-up system, which included not only contaminants (H_2S, siloxanes) removal but also biogas de-humidification and eventually pressurization. The importance of a reduced cost for cleaning units in fuel cell application is strongly underlined by manufacturers and utilities in [38] and is confirmed by the economic performance shown in Table 13. In the current SOFC cost scenario, PBT is kept high despite the clean-up cost reduction while, if the same analysis is performed with more competitive SOFC prices, the influence of clean-up strongly increases.

As discussed, more than 50% of the total plant investment cost is due to the SOFC, in particular, SOFC stack manufacturing and assembly are very cost intensive. Production volumes are the

main driver to reduce stack cost, and their effect is shown in Table 12 (the sensitivity has been performed for the base case 1). By moving from 1 to 2 MW/yr of production volumes, PBT is reduced of around 3 times (from 20 to 7.5) and with 5 MW/yr the system reaches competitive economic performance with a PBT lower than 4 years. A possible future work could be devoted to future scenarios with specific incentives: in fact, no subsidy has been considered in the analysis. Furthermore, despite the CHP technology analyzed, the WWTP high thermal demand is also a reason for the high operating cost of the system and increase the non-profitability of the fuel cell system in the current scenario.

6. Conclusion

Thermal and electric power needs for wastewater treatment are high, at the same time the process yields significant amounts of methane-containing biogas. Biogas is available from the anaerobic digestion of organic materials collected in sludge.

In this work, biogas-fed solid oxide fuel cell system is analyzed to contribute to the thermal and electrical needs of the medium-size WWTP. Real biogas and hourly sludge profiles were available from the WWTP and were used to define the plant size.

Scenarios were studied in which the thermal need of the digester is partially covered by additional heat recovered from solar collectors.

Results show, both on energy and on economic performance, the negative NG contribution due to the large digester thermal load not completely satisfied by the SOFC thermal recovery. For this reason, the choice of a solar installation results as a positive choice with a payback time of the isolated CST system investment of 9 years. The overall plant economic analysis shows that the technology still needs improvement to reduce clean-up and SOFC module specific costs, which are the main reasons for the high current pay-back time.

In the end, it can be stated that the results presented in this paper arise from our modeling activity within the DEMOSOFC project, which is a real application. Also, our results rely on experimental data (biogas availability, thermal and electrical demands) on the WWTP that will host the biogas-fed SOFC generators of the DEMOSOFC project. Therefore, we think there is a close link between results presented in this work and real-life application.

7. Acknowledgments

This project has received funding from the Fuel Cells and Hydrogen 2 Joint Undertaking under grant agreement Nº 671470 ‘DEMOSOFC (Demonstration of large SOFC systems fed with biogas from WWTP).' This Joint Undertaking receives support from the European Union’s Horizon 2020 research and innovation program.

SMAT S.p.a. is acknowledged for the sharing valuable data on the operation of Collegno (TO) WWTP.

Appendix

For modeling the SOFC system, we have considered the components as a control volume. The key component of the SOFC system is its stack. The molar conversion rates for the reforming, shifting and electrochemical reactions are indicated by x_r, y_r, and z_r, respectively as indicated by Eqs A1-A3.

$$x_r \rightarrow \left[CH_4 + H_2O \rightarrow CO + 3H_2\right] \quad \text{A1}$$

$$y_r \rightarrow \left[CO + H_2O \leftrightarrow CO_2 + H_2\right] \quad \text{A2}$$

$$z_r \rightarrow \left[H_2 + \frac{1}{2}O_2 \rightarrow H_2O\right] \quad \text{A3}$$

For given values of current density, Faraday's constant, cell number, and active surface area, the Z_r can be calculated using the following equation [42]:

$$z_r = \frac{j \cdot N_{FC} \cdot A_a}{2 \cdot F} \quad \text{A4}$$

Considering the mass balance equations (See Table A1), there should be three more equations to solve the system of equations. Two additional equations come from equilibrium constants for the shift and reforming reactions. These equations are as follows [42]:

Table A1. Mass balance for the SOFC stack.

Anode Side	$\dot{n}_{CH_4,9} = \dot{n}_{CH_4,8} - x_r$; $\dot{n}_{CO_2,9} = \dot{n}_{CO_2,8} + y_r$; $\dot{n}_{CO,9} = \dot{n}_{CO,8} + x_r - y_r$ $\dot{n}_{H_2O,9} = \dot{n}_{H_2O,8} - x_r - y_r + z_r$; $\dot{n}_{H_2,9} = \dot{n}_{H_2,9} + 3x_r + y_r - z_r$ $\dot{n}_8 = \dot{n}_{H_2,8} + \dot{n}_{CO_2,8} + \dot{n}_{H_2O,8} + \dot{n}_{CO,8} + \dot{n}_{CH_4,8}$ $\dot{n}_9 = \dot{n}_{H_2,9} + \dot{n}_{CO_2,9} + \dot{n}_{H_2O,9} + \dot{n}_{CO,9} + \dot{n}_{CH_4,9}$
Cathode side	$\dot{n}_{O_2,4} = \dot{n}_{O_2,3} - \frac{z_r}{2}$; $\dot{n}_{N_2,4} = \dot{n}_{N_2,3}$ $\dot{n}_3 = \dot{n}_{O_2,3} + \dot{n}_{N_2,3}$; $\dot{n}_4 = \dot{n}_{O_2,4} + \dot{n}_{N_2,4}$

$$\ln K_s = -\frac{\Delta \bar{g}_s^o}{\bar{R} T_{FC,e}} = \ln\left[\frac{(\dot{n}_{CO_2,9})\times(\dot{n}_{H_2,9})}{(\dot{n}_{CO,9})\times(\dot{n}_{H_2O,9})}\right] \quad \text{A5}$$

$$\ln K_R = -\frac{\Delta \bar{g}_R^o}{\bar{R} T_{FC,e}} = \ln\left[\frac{(\dot{n}_{CO,9})\times(\dot{n}_{H_2,9})^3}{(\dot{n}_{CH_4,9})\times(\dot{n}_{H_2O,9})\times \dot{n}_9^2}\left(\frac{P_9}{P_{ref}}\right)^2\right] \quad \text{A6}$$

where, $\bar{R}$ and $T_{FC,e}$ are the universal gas constant ($8.314\ \text{J.mole}^{-1}.\text{K}^{-1}$) and the temperature at the SOFC exit, respectively. The $\Delta \bar{g}^o$ for the shift and reforming reactions can be written as;

$$\Delta \bar{g}_s^o = \bar{g}_{s,CO_2}^o + \bar{g}_{s,H_2}^o - \bar{g}_{s,H_2O}^o - \bar{g}_{s,CO}^o \quad \text{A7}$$

$$\Delta \bar{g}_R^o = \bar{g}_{R,CO}^o + \bar{g}_{R,H_2}^o - \bar{g}_{R,H_2O}^o - \bar{g}_{R,CO_4}^o \quad \text{A8}$$

where,

$$\bar{g}^o = \bar{h} - T_{FC,e}\bar{s}^o \quad \text{A9}$$

In Eq. (A9) $\bar{h}$ and $\bar{s}^o$ are the molar enthalpy and absolute molar entropy, respectively. For ideal gases, $\bar{h}$ is function of temperature and $\bar{s}^o$ is a function of temperature and standard pressure.

The last equation needed for solving the system of equations is obtained using the energy balance for the whole stack. Neglecting the heat loss from the stack, the energy balance can be written as follows;

$$\dot{W}_{FC,stack} = \sum_k \dot{n}_{k,3}\bar{h}_{k,3} + \sum_L \dot{n}_{L,8}\bar{h}_{L,8} - \sum_m \dot{n}_{m,4}\bar{h}_{m,4} - \sum_n \dot{n}_{n,9}\bar{h}_{n,9} \quad \text{A10}$$

where, k, L, m and n are the gas mixture components in each state. On the other hand, the work rate produced by the SOFC stack, $\dot{W}_{FC,stack}$ can be expressed as;

$$\dot{W}_{FC,stack} = N_{FC}\cdot j \cdot A_a \cdot V_c \quad \text{A11}$$

The cell voltage, on the other hand, can be defined as;

$$V_c = V_N - V_{loss} \quad \text{A12}$$

where, V_N is the Nernst voltage and V_{loss} is the voltage loss which is the sum of three separate voltage losses (See Table A2):

$$V_{loss}=V_{ohm}+V_{act}+V_{conc} \quad \text{A13}$$

Table A2. Electrochemical equations used for calculating the Nernst voltage and voltage losses [43–45].

Voltage term	Equations
Nernst voltage	$V_N = -\frac{\Delta\bar{g}^o}{2F} + \frac{\bar{R}T_{FC}}{2F}\ln\left(\frac{a_{H_2}\sqrt{a_{O_2}}}{a_{H_2O}}\right)$; $a_{H_2}=\frac{P_{H_2}}{P_{ref}}$, $a_{H_2O}=\frac{P_{H_2O}}{P_{ref}}$, $a_{O_2}=\frac{P_{O_2}}{P_{ref}}$ $\Delta\bar{g}^o = \bar{g}^o_{H_2O} - \bar{g}^o_{H_2} - \frac{1}{2}\bar{g}^o_{O_2}$
Ohmic overvoltage	$V_{ohm} = j\ (\rho_{an}L_{an} + \rho_{cat}L_{cat} + \rho_{ely}L_{ely} + \rho_{int}L_{int})$ $L_{an} = 500\ \mu m\ ;\ L_{cat} = 50\ \mu m\ ;\ L_{ely} = 10\ \mu m\ ;\ L_{int} = 3000\ \mu m$ $\rho_{an} = 2.98\times10^{-5}e^{(\frac{-1392}{T})}\ [\Omega m]$ $\rho_{cat} = 8.114\times10^{-5}e^{(\frac{600}{T})}\ [\Omega m]$ $\rho_{ely} = 2.94\times10^{-5}e^{(\frac{10350}{T})}\ [\Omega m]$ $\rho_{int} = 0.0003215\ [\Omega m]$
Activation overvoltage	$V_{act} = V_{act,a} + V_{act,c}$; $V_{act,an} = \frac{2\bar{R}T_{FC}}{n_eF}(\sinh^{-1}(\frac{j}{2j_{o,an}}))$; $V_{act,cat} = \frac{2\bar{R}T_{FC}}{n_eF}(\sinh^{-1}(\frac{j}{2j_{o,cat}}))$ $j_{0,an} = \gamma_{an}\ (\frac{RT_{FC}}{2F})\,e^{\left(-\frac{E_{a,an}}{\bar{R}T_{FC}}\right)}$; $j_{0,cat} = \gamma_{cat}\ (\frac{RT_{FC}}{2F})\,e^{\left(-\frac{E_{a,cat}}{\bar{R}T_{FC}}\right)}\ [\frac{A}{m^2}]$ $\gamma_{an} = 6.54\times10^{11}\ [\frac{A}{m^2}]$; $\gamma_{cat} = 2.35\times10^{11}\ [\frac{A}{m^2}]$ $E_{a,An} = 140000\ [\frac{kJ}{kmol}]\ E_{a,Cat} = 137000\ [\frac{kJ}{kmol}]$
Concentration overvoltage	$V_{conc}=V_{conc,a}+V_{conc,c}$; $V_{conc,an} = \frac{RT_{FC}}{2F}\ln(\frac{P_{H_2}\ P_{H_2O,TPB}}{P_{H_2O}\ P_{H_2,TPB}})$; $V_{conc,cat} = \frac{RT_{FC}}{4F}\log(\frac{P_{O_2}}{P_{O_2,TPB}})$ $P_{H_2O,TPB} = P_{H_2O,an} + j\frac{R\,T_{FC}\,L_{an}}{2\,F\,D^{eff}_{an,H_2}}$; $P_{H_2,TPB} = P_{H_2,an} - j\frac{R\,T_{FC}\,L_{an}}{2\,F\,D^{eff}_{an,H_2O}}$ $P_{O_2,TPB} = P_{cat} - (P_{cat} - P_{O_2,cat})\exp(j\frac{RT_{FC}\,L_{cat}}{4F\,D^{eff}_{O_2}\,p_{cat}})$

$$\frac{1}{D_{an,H_2}^{eff}}=\frac{\varepsilon_{an}}{\tau_{an}}(\frac{1}{D_{H_2,K}}+\frac{1}{D_{H_2,H_2O}});\quad \frac{1}{D_{an,H_2O}^{eff}}=\frac{\varepsilon_{an}}{\tau_{an}}(\frac{1}{D_{H_2O,K}}+\frac{1}{D_{H_2O,H_2}})$$

$$\frac{1}{D_{\mathrm{cat},O_2}^{eff}}=\frac{\varepsilon_{cat}}{\tau_{cat}}(\frac{1}{D_{O_2,K}}+\frac{1}{D_{O_2,N_2}})$$

$$D_{H_2,K}=97\,r_{pore,an}\sqrt{\frac{T_{FC}}{M_{H_2}}};D_{H_2O,K}=97\,r_{pore,an}\sqrt{\frac{T_{FC}}{M_{H_2O}}};\ D_{O_2,K}=97\ r_{pore,cat}\sqrt{\frac{T_{FC}}{M_{O_2}}}\ [\frac{m^2}{s}]$$

$$D_{H_2,H_2O}=\frac{1.43\times10^{-7}T_{FC}^{1.75}}{\sqrt{M_{H_2,H_2O}}(\mathrm{V}_{\mathrm{H_2}}^{1/3}+\mathrm{V}_{\mathrm{H_2O}}^{1/3})^2P};\ D_{O_2,N_2}=\frac{1.43\times10^{-7}T_{FC}^{1.75}}{\sqrt{M_{O_2,N_2}}(\mathrm{V}_{O_2}^{1/3}+\mathrm{V}_{N_2}^{1/3})^2P}\,[\frac{m^2}{s}]$$

The porosity (ε) and tortuosity (τ) of electrode materials are estimated to be 0.48 and 5.4, respectively; meanwhile pore radius values are considered to be 0.5 μm [43]. Note that, calculation based parameters for activation overvoltage (Pre-exponential factor and Activation energy values for anode and cathode are taken from Refs. [44,45]

For the rest of components, molar balance and energy balance equations are provided in Table A3. The validation for the stack of SOFC system is given in our previously published work [46].

Table A3. Molar and energy balance equations for the components of the proposed SOFC system

Component	Molar balance	Energy balance
Air blower	$\dot{n}_1=\dot{n}_{air}$; $\dot{n}_1=\dot{n}_{N_2,1}+\dot{n}_{O_2,1}$; $\dot{n}_1=\dot{n}_2$	$\dot{W}_{Air,Blower}=\dot{n}_2\overline{h}_2-\dot{n}_1\overline{h}_1$
Fuel blower	$\dot{n}_5=\dot{n}_{biogas}+\dot{n}_{NG}$; $\dot{n}_5=\dot{n}_{CH_4,5}+\dot{n}_{CO_2,5}$	$\dot{W}_{Fuel,Blower}=\dot{n}_5\overline{h}_5-(\dot{n}_{5a}\overline{h}_{5a}+\dot{n}_{5b}\overline{h}_{5b})$
Air preheater	$\dot{n}_2=\dot{n}_3$; $\dot{n}_{13}=\dot{n}_{14}$ $\dot{n}_{13}=\dot{n}_{CO_2,13}+\dot{n}_{H_2O,13}+\dot{n}_{O_2,13}+\dot{n}_{N_2,13}$	$\dot{Q}_{AHX}=\dot{n}_3\overline{h}_3-\dot{n}_2\overline{h}_2$ $\dot{Q}_{AHX}=\dot{n}_{13}\overline{h}_{13}-\dot{n}_{14}\overline{h}_{14}$
Fuel HX	$\dot{n}_7=\dot{n}_8$; $\dot{n}_9=\dot{n}_{10}$ $\dot{n}_7=\dot{n}_{CO,7}+\dot{n}_{CO_2,7}+\dot{n}_{H_2O,7}+\dot{n}_{H_2,7}+\dot{n}_{CH_4,7}$ $\dot{n}_9=\dot{n}_{CO,9}+\dot{n}_{CO_2,9}+\dot{n}_{H_2O,9}+\dot{n}_{H_2,9}+\dot{n}_{CH_4,9}$	$\dot{Q}_{FHX}=\dot{n}_8\overline{h}_8-\dot{n}_7\overline{h}_7$ $\dot{Q}_{FHX}=\dot{n}_9\overline{h}_9-\dot{n}_{10}\overline{h}_{10}$
Pre-reformer	$\dot{n}_{CH_4,7}=\dot{n}_{CH_4,6}-p_r$ $\dot{n}_{H_2,7}=\dot{n}_{H_2,6}+3p_r+q_r$ $\dot{n}_{H_2O,7}=\dot{n}_{H_2O,6}-p_r-q_r$ $\dot{n}_{CO,7}=\dot{n}_{CO,6}+p_r-q_r$ $\dot{n}_{CO_2,7}=\dot{n}_{CO_2,6}+q_r$	$\dot{n}_6\overline{h}_6+\dot{Q}_{PR}=\dot{n}_7\overline{h}_7$

	$\ln K_{s,PR} = -\frac{\Delta \bar{g}^{o}_{s,PR}}{\bar{R}T_{PR}} = \ln\left[\frac{(\dot{n}_{CO_2,7})\times(\dot{n}_{H_2,7})}{(\dot{n}_{CO,7})\times(\dot{n}_{H_2O,7})}\right]$ $\ln K_{R,PR} = -\frac{\Delta \bar{g}^{o}_{R,PR}}{\bar{R}T_{PR}} = \ln\left[\frac{(\dot{n}_{CO,7})\times(\dot{n}_{H_2,7})^3}{(\dot{n}_{CH_4,7})\times(\dot{n}_{H_2O,7})\times \dot{n}_7^2}\left(\frac{P_7}{P_{ref}}\right)^2\right]$	
After burner	$\dot{n}_{CO_2,13} = \dot{n}_{CO_2,12} + \dot{n}_{CO,12}$ $\dot{n}_{H_2O,13} = \dot{n}_{H_2O,12} + \dot{n}_{H_2,12}$ $\dot{n}_{O_2,13} = \dot{n}_{O_2,4} - \frac{1}{2}\dot{n}_{H_2,12} - \frac{1}{2}\dot{n}_{CO,12}$ $\dot{n}_{N_2,13} = \dot{n}_{N_2,4}$	$\eta_{AB} = \frac{\dot{n}_{13}\bar{h}_{13}}{\dot{n}_{12}\bar{h}_{12} + \dot{n}_4\bar{h}_4}$
Mixer	$\dot{n}_{11} + \dot{n}_5 = \dot{n}_6$	$\dot{n}_{11}\bar{h}_{11} + \dot{n}_5\bar{h}_5 = \dot{n}_6\bar{h}_6$
Splitter	$\dot{n}_{11} + \dot{n}_{12} = \dot{n}_{10}$	$\bar{h}_{11} = \bar{h}_{12} = \bar{h}_{10}$

References

[1] 2050 Energy strategy - European Commission n.d.

[2] Madi H, Diethelm S, Poitel S, Ludwig C, Van herle J. Damage of Siloxanes on Ni-YSZ Anode Supported SOFC Operated on Hydrogen and Bio-Syngas. Fuel Cells 2015;15:718–27. doi:10.1002/fuce.201400185.

[3] Madi H, Lanzini A, Diethelm S, Papurello D, Van herle J, Lualdi M, et al. Solid oxide fuel cell anode degradation by the effect of siloxanes. J Power Sources 2015;279:460–71. doi:10.1016/j.jpowsour.2015.01.053.

[4] Papadias DD, Ahmed S, Kumar R. Fuel quality issues with biogas energy - An economic analysis for a stationary fuel cell system. Energy 2012;44:257–77. doi:DOI 10.1016/j.energy.2012.06.031.

[5] Eastern Research Group Inc., Analysis E and E. Opportunities for Combined Heat and Power at Wastewater Treatment Facilities : Market Analysis and Lessons from the Field Combined Heat and Power Partnership. US EPA, CHP Partnersh 2011:57.

[6] Tjaden B, Gandiglio M, Lanzini a., Santarelli M, Järvinen M. Small-scale biogas-SOFC plant: Technical analysis and assessment of different fuel reforming options. Energy and Fuels 2014;28:4216–32. doi:10.1021/ef500212j.

[7] Panepinto D, Fiore S, Zappone M, Genon G, Meucci L. Evaluation of the energy efficiency of a large wastewater treatment plant in Italy. Appl Energy 2016;161:404–11. doi:10.1016/j.apenergy.2015.10.027.

[8] CWW. Evaluation of Combined Heat and Power Technologies for Wastewater Facilities 2012:244.

[9] FuelCell Energy Inc. “FuelCell Energy: Ultra Clean, Efficient, Reliable Power” 2015.

[10] Lanzini a., Kreutz TG, Martelli E, Santarelli M. Energy and economic performance of novel integrated gasifier fuel cell (IGFC) cycles with carbon capture. Int J Greenh Gas Control 2014;26:169–84. doi:10.1016/j.ijggc.2014.04.028.

[11] Pellegrino S, Lanzini A, Leone P. Techno-economic and policy requirements for the market-entry of the fuel cell micro-CHP system in the residential sector. Appl Energy 2015;143:370–82. doi:10.1016/j.apenergy.2015.01.007.

[12] Margalef P, Brown T, Brouwer J, Samuelsen S. Efficiency of poly-generating high temperature fuel cells. J Power Sources 2011;196:2055–60. doi:10.1016/j.jpowsour.2010.10.046.

[13] Margalef P, Brown T, Brouwer J, Samuelsen S. Conceptual design and configuration performance analyses of polygenerating high temperature fuel cells. Int J Hydrogen Energy 2011;36:10044–56. doi:10.1016/j.ijhydene.2011.05.072.

[14] Sanchez D, Monje B, Chacartegui R, Campanari S. Potential of molten carbonate fuel cells to enhance the performance of CHP plants in sewage treatment facilities 2012;8. doi:10.1016/j.ijhydene.2012.09.145.

[15] Rinaldi G, McLarty D, Brouwer J, Lanzini A, Santarelli M. Study of CO2 recovery in a carbonate fuel cell tri-generation plant. J Power Sources 2015;284:16–26. doi:10.1016/j.jpowsour.2015.02.147.

[16] Trendewicz AA, Braun RJ. Techno-economic analysis of solid oxide fuel cell-based combined heat and power systems for biogas utilization at wastewater treatment facilities. J Power Sources 2013;233:380–93.

[17] Borello D, Evangelisti S TE. Modeling of a CHP SOFC System Fed with Biogas from Anaerobic Digestion of Municipal Waste Integrated with Solar Collectors and Storage Unit. Int J Thermodyn 2013;16 (1):28–35.

[18] de Arespacochaga N, Valderrama C, Peregrina C, Mesa C, Bouchy L, Cortina JL. Evaluation of a pilot-scale sewage biogas powered 2.8 kWe Solid Oxide Fuel Cell: Assessment of heat-to-power ratio and influence of oxygen content. J Power Sources 2015;300:325–35. doi:10.1016/j.jpowsour.2015.09.086.

[19] Papurello D, Borchiellini R, Bareschino P, Chiodo V, Freni S, Lanzini A, et al. Performance of a Solid Oxide Fuel Cell short-stack with biogas feeding. Appl Energy 2014;125:254–63. doi:10.1016/j.apenergy.2014.03.040.

[20] Papurello D, Lanzini A, Tognana L, Silvestri S, Santarelli M. Waste to energy: Exploitation of biogas from organic waste in a 500 Wel solid oxide fuel cell (SOFC) stack. Energy 2015;85:145–58.

[21] Buonomano A, Calise F, Ferruzzi G, Palombo A. Molten carbonate fuel cell: An experimental analysis of a 1kW system fed by landfill gas. Appl Energy 2015;140:146–60. doi:10.1016/j.apenergy.2014.11.044.

[22] Chiodo V, Galvagno a., Lanzini a., Papurello D, Urbani F, Santarelli M, et al. Biogas reforming process investigation for SOFC application. Energy Convers Manag 2015;98:252–8. doi:10.1016/j.enconman.2015.03.113.

[23] Http://www.sofcom.eu. SOFCOM Project, SOFC CCHP with Poly-fuel Operation and Maintenance n.d.

[24] Gandiglio M, Lanzini A, Santarelli M, Leone P. Design and balance of plant of a demonsration plant with a Solid Oxide Fuel Cell fed by biogas from Waste-water and exhaust carbon recycling for algae growth. J Fuel Cell Sci Technol 2013;11:14. doi:10.1115/FuelCell2013-18082.

[25] DEMOSOFC project official website n.d.

[26] Cheremisinoff NP. Handbook of Water and Wastewater Treatment Technologies. 2002.

[27] Akkaya AV, Sahin B, Huseyin Erdem H. An analysis of SOFC/GT CHP system based on exergetic performance criteria. Int J Hydrogen Energy 2008;33:2566–77. doi:10.1016/j.ijhydene.2008.03.013.

[28] Wu X-J, Zhu X-J. Multi-loop control strategy of a solid oxide fuel cell and micro gas turbine hybrid system. J Power Sources 2011;196:8444–9. doi:10.1016/j.jpowsour.2011.05.075.

[29] Yari M, Mehr AS, Mahmoudi SMS. Thermodynamic analysis and optimization of a novel dual-evaporator system powered by electrical and solar energy sources. Energy 2013;61:646–56. doi:10.1016/j.energy.2013.09.025.

[30] Rayegan R, Tao YX. A procedure to select working fluids for Solar Organic Rankine Cycles (ORCs). Renew Energy 2011;36:659–70. doi:10.1016/j.renene.2010.07.010.

[31] National Renewable Energy Laboratory (NREL). System advisor model (SAM). n.d.

[32] Pizza F. Welcome to Milano-Nosedo municipal WWTP The WWTP of Milano Nosedo 2015.

[33] Mazzini R. Calore per riscaldamento dalle acque reflue della citta', 2014.

[34] Gse. Incentivazione della produzione di energia elettrica da impianti a fonti rinnovabili diversi dai fotovoltaici. WwGseIt 2012:1–139.

[35] Curletti F, Gandiglio M, Lanzini A, Santarelli M. Large size biogas-fed Solid Oxide Fuel Cell power plants with carbon dioxide management : Technical and economic optimization 2015;294.

[36] Agenzia delle Entrate. Income tax for individuals n.d.

[37] International Energy Agency. Projected Costs of Generating Electricity. 2010.

[38] Argonne National Laboratory. Gas Clean-Up for Fuel Cell Application Workshop 2014:1–32.

[39] DOE NETL, Thjissen J. The Impact of Scale-Up and Production Volume on SOFC Manufacturing Cost 2007.

[40] Roland Berger Strategy Consultants. Advancing Europe's energy systems: Stationary fuel cells in distributed generation. A study for the Fuel Cells and Hydrogen Joint Undertakinng. 2015. doi:10.2843/088142.

[41] Turton R, Bailie RC, Wniting WB, Shaeiwitz A, Eclition T. Analysis, Synthesis and Design of Chemical Processes. n.d.

[42] Mehr AS, Mahmoudi SMS, Yari M, Chitsaz A. Thermodynamic and exergoeconomic analysis of biogas fed solid oxide fuel cell power plants emphasizing on anode and cathode recycling: A comparative study. Energy Convers Manag 2015;105:596–606.

[43] Wongchanapai S, Iwai H, Saito M, Yoshida H. Selection of suitable operating conditions for planar anode-supported direct-internal-reforming solid-oxide fuel cell. J Power Sources 2012;204:14–24.

[44] P. Aguiar, C.S. Adjiman NPB. Anode-supported intermediate temperature direct internal reforming solid oxide fuel cell. I: model-based steady-state performance. J Power Sources 2004;138:120–36.

[45] Z. Bariza, G.M. Andreadis MH Ben. Two-dimensional numerical study of temperature field in an anode supported planar SOFC: Effect of the chemical reaction. Int J Hydrogen Energy 2011;136:4228–35.

[46] Yari M, Mehr AS, Mahmoudi SMS, Santarelli M. A comparative study of two SOFC based cogeneration systems fed by municipal solid waste by means of either the gasifier or digester. Energy 2016;114:586–602. doi:10.1016/j.energy.2016.08.035.